RESEARCH
ENGINEERING
RESEARCH
ENGINEERING
RESEARCH
ENGINEERING

ENGINEERING
RESEARCH
INSTITUTE

IOWA STATE
UNIVERSITY
AMES, IOWA

Progress Report

Performance Tests for the NASA Ames Research Center 20 cm x 40 cm Oscillating Flow Wind Tunnel

William J. Cook, Professor
Department of Mechanical Engineering
and
Tim A. Giddings, Graduate Student
Department of Mechanical Engineering

December 31, 1984

ENGINEERING
RESEARCH
ENGINEERING
RESEARCH

ISU-ERI-Ames-85436

Progress Report for the period June 1, 1984 to December 31, 1984
Project 1601

Submitted to the NASA Ames Research Center under
Grant No. NCC2-200 entitled "Study of
Turbulent Boundary Layers in Oscillating Flows"
W. J. Cook, Principal Investigator
J. D. Murphy, Grant Technical Monitor

Progress Report

Performance Tests for the NASA Ames Research Center 20 cm x 40 cm Oscillating Flow Wind Tunnel

William J. Cook, Professor
Department of Mechanical Engineering
and
Tim A. Giddings, Graduate Student
Department of Mechanical Engineering

December 31, 1984

engineering research institute
iowa state university COLLEGE OF ENGINEERING, AMES, IOWA 50011

TABLE OF CONTENTS

NOMENCLATURE

a	sonic velocity
C_L	centerline
C_f	friction coefficient, $\tau_w/[\frac{1}{2}\rho U_o^2]$
f	frequency, Hz
H	boundary layer shape factor, δ^*/θ
ℓ	test section length
M_o	mean Mach number, U_o/a
Re_θ	Reynolds number based on momentum thickness
Re_x	Reynolds number based on x
S	Mach number variation, equations (5) and (5a)
t	time
u	x component of boundary layer velocity, ensemble average
u'	fluctuating component of velocity
u^+	u/u_τ
u_τ	friction velocity, $[\tau_w/\rho]^{\frac{1}{2}}$
U	mainstream velocity, ensemble average
U_c	centerline velocity, Figure 3
x	axial distance measured from test section entrance
y	distance perpendicular to test section wall
y^+	yu_τ/ν
β	phase angle, equation (6)
δ	steady flow velocity boundary layer thickness
δ^*	displacement thickness
θ	momentum thickness, phase angle, equation (5) and (5b)
μ	coefficient of viscosity
ν	μ/ρ
ρ	density
τ_w	wall shear stress
ϕ	phase angle, equation (7)
ω	angular frequency, radians/sec
$\bar{\omega}$	reduced frequency, $\omega x/U_o$

Subscripts:

o	mean velocity based on ensemble average
1	amplitude of velocity variation based on ensemble averaged values

Performance Tests for the NASA Ames Research Center 20 cm x 40 cm Oscillating Flow Wind Tunnel

W. J. Cook[†] and Tim A. Giddings[*]
Iowa State University, Ames, Iowa

SUMMARY

This report describes and presents an evaluation of initial tests conducted to assess the performance of the NASA Ames 20 cm x 40 cm oscillating flow wind tunnel. The features of the tunnel are described and two aspects of tunnel operation are discussed. The first is an assessment of the steady mainstream and boundary layer flows and the second deals with oscillating mainstream and boundary layer flows. Experimental results indicate that in steady flow the test section mainstream velocity is uniform in the flow direction and in cross section. The freestream turbulence intensity is about 0.2 percent. With minor exceptions the steady turbulent boundary layer generated on the top wall of the test section exhibits the characteristics of a zero pressure gradient turbulent boundary layer generated on a flat plate. The tunnel was designed to generate sinusoidal oscillating mainstream flows. Experiments confirm that the tunnel produces sinusoidal mainstream velocity variations for the range of frequencies investigated (up to 15 Hz). The mainstream flows were observed to vary in amplitude and phase in the direction of flow in the upper range of frequency, as predicted qualitatively by theory. The oscillating flow boundary layer case studied indicates that boundary layer flows similar to those observed in other oscillating flow experiments are generated in the tunnel. The results of this study demonstrate that the tunnel essentially produces the flows that it was designed to produce.

INTRODUCTION

The NASA Ames 20 cm x 40 cm oscillating flow wind tunnel is located in the Aerodynamics Research Branch of the Ames Research Center. Its design is based on a smaller tunnel which is described in References 1, 2, and 3. The facility was first operated in July of 1984. This report describes and presents an evaluation of initial tests performed in July and August of 1984 to assess the performance of the tunnel. Two aspects of tunnel operation are covered. The first is an assessment of the steady mainstream and boundary layer flows produced. The second part reports results for oscillating flow experiments for both mainstream and boundary layer flow.

[†]Professor, Mechanical Engineering and Engineering Research Institute

[*]Graduate student, Mechanical Engineering Department

FACILITY DESCRIPTION

The 20 cm x 40 cm oscillating flow tunnel is described in Figure 1 and Table 1. The facility is vacuum driven by means of a line connected to the Ames Research Center Unitary Wind Tunnel vacuum system. Room air flows into the test section through the entrance section which has an area contraction ratio of 9 to 1. The honeycomb and screens in the entrance section are described in Table 1. The test section is nominally 20 cm high and 40 cm wide, in cross section and is 2.75 m in length. The walls are 2.54 cm thick Plexiglas. The vertical walls diverge in the direction of flow to produce zero pressure gradient flow when the flow is steady. Instrument ports are provided on the top and bottom walls at several axial locations along the centerlines over the length of the test section. In addition, sliding wall segments are provided on the top and bottom walls at distances 0.15 m and 1.88 m from the test section entrance for surveys in the transverse (z) direction.

During operation, the nozzle discharge-region pressure is low enough to maintain sonic flow at the nozzle throat. When the position of the wedge in the wave generator section is fixed, the test section flow is steady. When the wave generator is operated at a fixed frequency, the test section mainstream flow velocity U is characterized by a mean velocity and a superposed oscillating component of the form

$$U(x,t) = U_o + U_1(x)\,\mathrm{Cos}\,\omega t \qquad (1)$$

where U_o is the mean velocity and U_1 is the half amplitude of the velocity variation, and ω is the angular frequency of the wave generator input shaft. The mean and oscillating velocity components for the test section flow can be selected within certain limits by choice of the nozzle throat cross section, the wedge leading-edge included angle, and the wedge stroke. The throat cross section can be altered by changing the nozzle throat blocks

shown in Figure 1. Two sets of blocks were used in the present tests. These are designated as nozzle block sets A and B and are described in Table 1. A single wedge with an included leading-edge angle of 20 degrees was used. Table 2 describes the wave generator configurations used in obtaining the results reported here. The unit Reynolds numbers for the flows associated with these configurations are such that natural transition from laminar to turbulent flow would occur in the test section wall boundary layers. Since it was desired to study turbulent boundary layers on the facility walls, boundary layer trip wires 0.63 mm in diameter were positioned on the four walls at the test section entrance to produce boundary layer transition. The wire diameter was chosen to produce transition at the trip[4].

A hot wire anemometer system was used as the primary means of obtaining data. Figure 2 describes the anemometer and the data acquisition system. The complete system was calibrated with the hot wire outside the tunnel using a TSI Model 1125 air flow calibrator and standard calibration techniques. All results reported here are based on measurements made through instrument ports on the top wall of the tunnel.

STEADY FLOW EXPERIMENTS

Studies of the flows associated with wave generator configurations I and II in Table 2 were conducted to examine both the mainstream and boundary layer flows produced in the tunnel under steady flow conditions. For steady flows, the data acquisition system, Figure 2, was programmed to take 500 hot wire voltage readings over a 1.5 second time span. Due to minor temperature changes, system drift, and hot wire contamination due to dust in the test air, it was necessary to check the hot wire calibration and make appropriate adjustments before each run. This was accomplished with the tunnel running by positioning the hot wire probe to a calibration point in the mainstream

flow and adjusting the system to display the calibration voltage. The average velocity and the RMS turbulence was determined by computer processing the 500 voltage readings. The uncertainty associated with the velocity measurements was estimated to be ± 1 percent*.

Steady Mainstream Flows

The mainstream flows were studied by means of velocity and static pressure measurements. Due to the divergence of the vertical test section walls to account for boundary layer displacement effects, the pressure drop over the length of the test section was essentially zero for the steady flows associated with wave generator configurations I and II. Correspondingly, there was no measureable change in the mainstream centerline velocity over the test section length for either flow. Measured values for the centerline velocities and the test section static pressures are given in Table 2 as are the corresponding unit Reynolds numbers.

Surveys of the velocity at x = 1.88 m over one half of the test section cross section were made for the flows produced by wave generator configuration I in order to examine the uniformity of the flow. The results are presented in Figure 3. Surveys were made at three values of y in the upper half of the test section as indicated in the figure and were confined to the flow region outside the boundary layers. The results are presented in terms of U/U_c vs z, where U_c is the average of two separate velocity measurements made on the axial centerline at x = 1.88 m. The results indicate that the mainstream flow is uniform within ± 2 percent variation from the centerline velocity in the region surveyed. The scatter in the results at a given value of y is related to the uncertainty of ± 1 percent in the velocity measurements.

*Uncertainties in this report are given as estimates of ± one standard deviation.

Steady Boundary Layer Flows

Velocity surveys were made for the boundary layer on the top wall at several axial locations for wave generator configurations I and II in Table 2 (steady flows). The first results to be discussed are those obtained from surveys made along the top wall centerline.

Velocity profiles u vs y were obtained using the data acquisition system, Figure 2, and were processed by means of a boundary layer analysis computer code provided by Westphal[5] to determine various boundary layer parameters. Figure 4 shows descriptive boundary layer quantities related to the flows for both wave generator configurations. Figure 4a displays the variation with x of the momentum-thickness Reynolds number Re_θ, the Ludwieg-Tillmann skin friction coefficient C_f given by[6]

$$C_f = \tau_w/[\tfrac{1}{2}\rho U_o^2] = 0.246\times10^{-0.678H}\, Re_\theta^{-0.268} \qquad (2)$$

and the boundary layer shape factor $H = \delta^*/\theta$. Bars indicating the estimated experimental uncertainty for Re_θ are shown. The uncertainties for C_f and H are approximately the symbol size. For the most part the results in Figure 4a exhibit the trends expected for a turbulent flat plate boundary layer. However, the value of Re_θ at x = 1.66 m, Configuration I, lies above the curve fitted through the remaining points. A possible explanation of this is that a test section joint lies 13 cm upstream of the instrument port at x = 1.66 m and joint mismatch may have been present and produced a local disturbance in the flow.

Figure 4b displays velocity boundary layer thicknesses δ for the flows related to each wave generator configuration. The symbols indicate values determined from experimental velocity profiles at 99 percent of the boundary layer edge velocity. Bars indicating the estimated experimental uncertainty in δ are shown. Also shown are curves based on the equation

$$\frac{\delta}{x} = 0.371\ Re_x^{-0.2} \qquad (3)$$

which predicts the velocity boundary layer thickness for turbulent flows over a flat plate. The predicted variation fits the experimental results for configuration I well, yielding the expression

$$\delta,\ cm = 1.888(x,\ m)^{0.8} \qquad (3a)$$

However, the experimental results for configuration II lie somewhat below the curve given by equation (3). The curve fitted through the points for configuration II is given by

$$\delta,\ cm = 1.72(x,\ m)^{0.8} \qquad (3b)$$

This result is somewhat anomalous since a thicker boundary layer should be associated with the lower mainstream velocity produced by configuration II. Possibly boundary layer transition did not occur at the trip wire.

Figures 5a and 5b present experimental velocity profiles in terms of u/U_o and y/δ for the steady flows related respectively to wave generator configurations I and II. Values of δ used in preparing these and subsequent figures involving δ were determined by use of equations (3a) and (3b) respectively. The several profiles in both Figures 5a and 5b exhibit essential agreement. Figure 5c compares the velocity profiles at x = 1.35 m and x = 2.48 m for the two flows. While the profiles agree very well for the two positions within either flow, a difference exists between the profiles for the two flows.

Figures 6a and 6b present boundary layer profile results in terms of u^+ vs y^+ for the two flows. The bars indicate the experimental uncertainty for the results at x = 0.44 m, where the uncertainty is the largest. The uncertainty at x = 2.48 m is approximately the symbol size. The uncertainties result from uncertainties in the freestream velocity. The results for these figures were obtained using C_f values predicted by equation (2). The collec-

tive profiles exhibit good agreement with the logarithmic law equation at the lower values of y^+, with the possible exception of the results at x = 0.44 m, Figure 6b. For this case, the turbulent boundary layer may not have been sufficiently developed, as indicated by the relatively small value of Re_θ (Re_θ = 2000, see Figure 4a).

Figures 7a and 7b show percent turbulence intensity defined as

$$\text{Turbulence intensity, percent} = 100[\overline{u'^2}]^{\frac{1}{2}}/u_o \qquad (4)$$

for the two flows: u' is the fluctuating component of velocity and u_o is the local velocity in the boundary layer. The results for turbulence intensity in these figures were obtained by computer processing of the 500 hot wire voltage readings taken at each y value using the data acquisition system. Although some scatter exists, results for the several x locations group fairly closely in both Figures 7a and 7b. Values of freestream turbulence intensity as indicated by the computer-acquired data are approximately 0.4 percent for both flows. Turbulence intensities were also measured by means of a Disa 55D35 true RMS meter operated in conjunction with a Disa 55D26 signal conditioner functioning as a 10 kHz low-pass filter to filter out high frequency noise present in the hot wire system. This noise introduced an error in turbulence intensity at very low values of turbulence intensity. Results obtained using these instruments were in essential agreement with those obtained from the computer-acquired data except in the region outside the boundary layer. Values of turbulence intensity measured in the mainstream with the RMS meter were in the range 0.16 to 0.20 percent.

Figure 7c shows a comparison of turbulence intensity profiles at x = 1.35 m and x = 2.48 m for steady flows produced by the two wave generator configurations. A difference in the two profiles for the two configurations is evident. Also shown for comparison purposes are turbulence intensity pro-

files measured in flat plate turbulent boundary layers at two freestream turbulence intensities, 0.02 percent and 0.3 percent[7, 8]. The experimental results for configuration I agree well with the curve for 0.3 percent turbulence intensity except at low values of y/δ where the results more closely agree with the curve for 0.02 percent turbulence intensity.

In addition to the top wall centerline boundary layer surveys discussed above, surveys were made at 11 cm each side of the top wall centerline at the x = 1.88 m axial location. Comparisons of some results from these surveys and the centerline survey at x = 1.88 m are presented in Figure 8. Figures 8a, 8b, and 8c show respectively velocity profiles, u^+ vs y^+, and turbulence intensity for the three surveys. In each of the figures the results for the three positions are essentially in agreement, indicating that a uniform turbulent boundary layer is developed across at least 22 cm of the 40 cm wide top wall.

Comments On Steady Flow Experiments

With minor exceptions, the experimental results indicate that the test section flows for steady operation of the tunnel are of good quality. The mainstream flows exhibit uniform velocity for the length of the test section and have relatively low freestream turbulence intensities, approximately 0.2 percent. Based on the good uniformity of the flow observed at the x = 1.88 m location, it is expected that the flow is equally uniform at other cross sections. The various boundary layer quantities described in Figures 4 through 8 indicate that turbulent boundary layers similar to those developed on flat plates with zero pressure gradient were generated on the tunnel top wall for each of the flows studied. However, the comparisons in Figures 5c and 7c show some differences between the boundary layers for configuration I

(U_o = 45.7 m/s) and those for configuration II (U_o = 26.6 m/s). These differences may be related to the fact that the boundary layer velocity thicknesses for configuration II flows are less rather than greater than those for configuration I. Use of larger values of δ for configuration II flows, as predicted by equation (3) results in very good agreement between the results for the two flows in both Figures 5c and 7c. However, as noted in Figure 4b, the values of δ determined from the experimental velocity profiles for configuration II do not justify the use of the prediction made directly from equation (3). Hence the fit in equation (3b) was used in preparing the curves involving y/δ for configuration II flows.

OSCILLATING FLOW EXPERIMENTS

Two aspects of oscillating flows produced by the tunnel were examined. The first dealt with the behavior of the mainstream oscillating flow and the second focused on one case of oscillating boundary layer flow. These are discussed separately below.

Mainstream Oscillating Flows

Previous experiments and theoretical analysis for mainstream flow for the present type of facility operated in the oscillating flow mode have shown that as frequency of oscillation increases from a low value, the amplitude of oscillation U_1 departs from uniformity with x and an x dependent phase difference denoted by θ appears in the flow (Refs. 1, 2, 3). The velocity variation with position and time at a fixed frequency of oscillation can be written for the mainstream as

$$U(x,t) = U_o + U_1(x)\mathrm{Cos}[\omega t + \theta(x)] \qquad (5)$$

$U_1(x)$ and $\theta(x)$ can be theoretically predicted from the following expressions.

$$U_1(x) = aS(x)$$

$$S(x) = \{(B\mathrm{Cos}\zeta + C\mathrm{Cosn}\zeta)^2 + (B\mathrm{Sin}\zeta - C\mathrm{Sinn}\zeta)^2\}^{\frac{1}{2}} \quad (5a)$$

$$\theta(x) = \tan^{-1}\{\frac{B\mathrm{Sin}\zeta - C\mathrm{Sinn}\zeta}{B\mathrm{Cos}\zeta + C\mathrm{Cosn}\zeta}\} \quad (5b)$$

where

$$n = \frac{1 - M_o}{1 + M_o}$$

$$\zeta = \frac{x\omega}{a\ (1 - M_o)}$$

In these expressions a is sonic velocity, $M_o = U_o/a$, and B and C are constants which are evaluated by use of two boundary conditions, the first of which is obtained at $x = \ell$. The ratio of A_ℓ, the area at the nozzle entrance, to the sonic area A* varies as A* changes due to the motion of the wedge. Neglecting the unsteady effects in the converging section of the nozzle and using the relation between A/A* and Mach number for isentropic flow, the Mach number variation $S(\ell)$ can be obtained from the wave generator geometry. The second boundary condition is obtained at $x = 0$. Unsteady effects are neglected in the entrance section and through a pressure matching iterative procedure, the second boundary condition is imposed. Since each boundary condition yields a relation between B and C, values for B and C are obtained.

Experiments related to the behavior of the mainstream flow in the present facility were conducted for frequencies ranging from 3 to 15 Hz. Velocity measurements using the data acquisition system, Figure 2, were made at $x = 0.11$ m and $x = 2.48$ m with the hot wire probe positioned through instrument ports on the top wall 6.7 cm from the wall. The same wave generator configuration was used for all oscillating flow experiments and is designated as configuration III in Table 2. The value of $S(\ell)$ for this configuration is 0.012. Hotwire voltage values were read at 20 equally

spaced time intervals for each cycle of oscillation. An external trigger to the voltmeter, Figure 2, was provided by the conditioned and amplified signal from a magnetic pickup, part of which was mounted on a flywheel fixed to the wave generator drive shaft. The shaft speed was controlled within 0.02 percent and was monitored by a light-sensing pickup and an EPUT counter. The 20 voltage readings per cycle were ensemble averaged over 100 cycles and converted to velocities by use of the hot wire calibration curve. A sine wave was then fitted to the 20 ensemble averaged velocity values. The resulting fits are of the form

$$U = U_o + U_1 \mathrm{Cos}(\omega t - \beta) \qquad (6)$$

where β is a phase angle. Figure 9a shows curves obtained in this manner for two frequencies of oscillation at x = 0.11 m and x = 2.48 m. Equations for the fitted curves are also shown. It is evident from the close proximity of the ensemble averaged results to the fitted curves that on an ensemble-averaged basis, the velocity variation is sinusoidal. At a frequency of 3 Hz the amplitude of oscillation U_1 at x = 0.11 m is slightly larger than that at x = 2.48 m, but U_o and β at the two locations are essentially the same. At 15 Hz, the results for the two positions show significantly different amplitudes of oscillation and exhibit a phase difference, with the oscillation at x = 2.48 m leading that at x = 0.11 m.

Results like those in Figure 9a can be displayed more descriptively in terms of S and θ vs x, as shown in Figure 9b. Experimental results at x = 0.11 m and 2.48 m as well as predicted variations for S and θ are displayed. At the lowest frequency, f = 3 Hz, S is predicted to be essentially constant with x at the value 0.012, indicating no significant variation in U_1 with x. A small variation in θ is also predicted. At higher frequencies, 15 Hz for example, larger variations in S and θ are predicted. It

is evident in the figure that most of the experimental values of S are larger that the corresponding predicted values. This can be seen more clearly in Figure 9c which compares predicted and experimental variations in S and θ in terms of frequency for the two x locations. While the trend for S is correctly predicted at x = 0.11 m, the variation in S indicated by the measurements at x = 0.11 m exhibits a more pronounced increase with frequency. This is probably related to the fact that the theory on which the prediction is based assumes that the facility has short entrance and subsonic nozzle section lengths compared to the test section length ℓ, a condition that does not exist in the present facility. Values of S at x = 2.48 m are larger than predicted values only for frequencies greater than 12 Hz. Also, as shown in the figure, the experimental results for θ at x = 2.48 m agree well with the predicted variation for $f \geq 10$ Hz. Experimental values in the remainder of the frequency range fall below the predicted curve. Apparently something not accounted for in the theory is taking place in the flow near the test section exit to produce these results.

Oscillating Boundary Layer Flows

A boundary layer survey was carried out for oscillating flow at the x = 1.66 m location on the top wall centerline at a frequency of 4.11 Hz for flows produced by wave generator configuration III. The reduced frequency $\overline{\omega} = \omega x/U_o$ for the flow produced is 0.96. Results at 12 values of y were obtained and are tabulated in Table 3. Data were taken in the manner described for the mainstream oscillating flow experiments. The number of cycles over which the 20 ensemble averaged velocity values were obtained is listed in the table. Sine waves were fitted to the 20 ensemble averaged velocity values for the cycle, yielding an equation of the form of equation

(6) at each of the 12 y values. The values of y/δ, as listed in Table 3, were obtained by dividing the y values by the steady flow boundary layer thickness at x = 1.66 m as given by equation (3a). Curves and the corresponding equations for the velocity variations at the extreme values of y/δ in the survey are shown in Figure 10a. The ensemble averaged velocity values closely fit the sine waves, even at the lowest value of y/δ at which data were taken.

With the freestream as a reference, the expression for the velocity in the boundary layer at a fixed x location can be written as

$$u(y,t) = u_o(y) + u_1(y)\text{Cos}[\omega t + \phi(y)] \qquad (7)$$

In the freestream $u_o = U_o$, $u_1 = U_1$ and $\phi = 0$. Values of u_o/U_o, u_1/U_1 and ϕ based on the listed values of U_o and U_1 are tabulated in Table 3. Figure 10b presents a comparison of mean velocity profiles in terms of u_o/U_o and y/δ. Shown are the steady flow profile at x = 1.66 m (Figure 5a), the profile for oscillating flows (Table 3) and the profile predicted by the numerical method developed by Murphy[9]. The Cebeci-Smith turbulence model[10] was used in obtaining the numerical predictions*. Also, δ as given in Table 3, was used to form the y/δ values for the numerical predictions in this and other related parts of Figure 10. The experimental oscillating flow velocity profile in Figure 10b agrees well with the experimental steady flow profile. However, the numerical method predicts values larger than the measured mean values in most of the boundary layer.

Figure 10c compares the experimental profile for u_1/U_1 from Table 3 with the numerically predicted profile. The results are in good agreement. Both indicate values of u_1/U_1 slightly larger than unity in a part of the boundary layer. Figure 10d shows a comparison of experimental results for the phase angle ϕ from Table 3 with those predicted numerically. The results

*The numerical predictions in Figure 10 were provided by J. D. Murphy.

are in reasonable agreement down to $y/\delta = 0.2$, after which experimental values for ϕ decrease while predicted values for ϕ increase. The same behavior was observed for a case with nearly the same reduced frequency for flows produced in a smaller-scale version of the present facility (Ref. 1). Results for this case as well as the present results are shown in Figure 10e. Since the same trend in experimental data was observed in both facilities at nearly the same flow conditions, there is a strong indication that the experimental behavior for ϕ observed at low values of y/δ is correct.

In the ensemble averaging process to obtain velocity values turbulence intensities were also computed at the 20 points in the cycle. Turbulence intensities as given by equation (4) with u_o replaced by the local ensemble averaged velocity were determined and a sine wave was fit to the 20 values to obtain a mean value and range of the turbulent intensity variation. Figure 10f shows a comparison of steady flow turbulence intensities and the turbulence intensities for oscillating flow. It is evident from the figure that except at values of y/δ greater than 1.1, the turbulence intensity for oscillating flow varies around a mean value equal to that for steady flow.

Comments on Oscillating Flow Experiments

The experimental results for oscillating flows clearly show that the mainstream velocity variation is sinusoidal for frequencies ranging up to 15 Hz. Further, the collective results for the mainstream oscillating flows as shown in Figure 9 indicate for the most part that the flow behaves qualitatively as predicted by the theory in that at higher frequencies the amplitude of oscillation decreases with increasing x and a phase difference exists between the downstream flow and the upstream flow, with the downstream flow leading the upstream flow. The influence of this feature of the flow on

boundary layer experiments at high frequencies, while unknown, is expected to be small. The ensemble averaged results for the oscillating boundary layer flow case studied show that at any point in the boundary layer the velocity oscillates sinusoidally around a mean value equal to that measured at the same point in the steady flow boundary layer. Similarly, the turbulence intensity for the oscillating flow varied around a mean value equal to that for steady flow. The observed values greater than unity for the amplitude ratio u_1/U_1 in the boundary layer are consistent with several other experiments. Also, the measured variation of phase angle for the case studied is consistent with results from a previous study of a similar flow in a smaller similar facility.

CONCLUDING REMARKS

Experiments performed to assess the flow in the 20 cm x 40 cm oscillating flow tunnel indicate that the facility produces good quality test flows when operated in either the steady flow mode or the oscillating flow mode. Results indicate that in steady flows, the mainstream velocity is uniform in the flow direction and in cross section. The freestream turbulence intensity is about 0.2 percent. With minor exceptions the steady turbulent boundary layer generated on the test section top wall exhibits the characteristics of a zero pressure gradient turbulent boundary layer generated on a flat plate. For oscillating flows the mainstream velocity variation is sinusoidal for frequencies up to 15 Hz, the highest frequency studied. These flows behave qualitatively as predicted by theory. The oscillating flow boundary layer case studied indicates that oscillating boundary layer flows like those observed in other oscillating flow experiments are generated in the tunnel. In conclusion, the results of this investigation indicate that the facility will provide an excellent experimental means of studying a number of aspects of viscous and inviscid oscillating flows.

REFERENCES

1. Cook, W. J. "A study of turbulent boundary layers in oscillating flows," Iowa State University Engineering Research Institute Technical Report ISU-ERI-Ames-84408, 1983.

2. Cook, W. J. and Yamaguchi, Y. "A faciltiy for studying turbulent boundary layers in oscillating flows," Iowa State University Engineering Research Institute Technical Report ISU-ERI-Ames-82186, 1982.

3. Cook, W. J. "A faciltiy for producing periodic subsonic flows," Iowa State University Engineering Research Institute Technical Report ISU-ERI-Ames-81117, 1980.

4. Smith, A. and Clutter, D. "The smallest height of rougness capable of affecting boundary layer transition," J. Aero. Sci., 26 (1959): 229-245.

5. Westphal, Russell "VPRO, A computer code for steady boundary layer data analysis," Private communication.

6. Coles, Donald "The young person's guide to the data," Poceedings, Computation of turbulent boundary layers, 1968 AFOSR-IFP-Stanford Conference, Vol. II, Stanford, CA, August 18-25, 1968.

7. Charnay, G., Comte-Rellot, G., and Mathien, J. "Development of a turbulent boundary layer on a flat plate in an external turbulent flow," AGARD-CP-93, London, U.K., Sept. 1971.

8. Schlichting H. "Boundary layer theory," 4th Edition, McGraw-Hill Book Company, New York. P. S. Kelvanoff results, p. 467.

9. Murphy, J. D. and Prenter, P. M. "A hybrid computing scheme for unsteady boundary layers," Third Symposium on Turbulent Shear Flows, University of California, Davis. 1981.

10. Cebeci, T. and Smith, A. M. O. "A finite difference solution of the imcompressibel turbulent boundary layer equations by an eddy-viscosity concept," AFOSR-IFP-Stanford Conference, 1968.

Table 1. Description of the 20 cm x 40 cm Oscillating Flow Tunnel. See Figure 1.

Entrance Section

Flow-Straightening Section: Cross Section, 0.62 m x 1.22 m
Length = 0.64 m

Contraction Section: Length = 1.22 m
Area Ratio = 9 to 1
Honeycomb: 0.32 cm Hex Cell x 2.54 cm
Screens (Listed in direction of Flow)

Mesh per inch	Porosity, %
10	64
20	64
30	60

Test Section

Length = 2.75 m

Cross Section:	Height	Width
Entrance,	20.3 cm	40.6 cm
Exit,	20.3 cm	43.8 cm

Material: 2.54 cm thick Plexiglas

Wave Generator

Length = 0.94 cm

Nozzle Throat Blocks:	Set A	Set B
Throat Cross Section,	10.2 cm x 20.3 cm	5.08 cm x 20.3 cm
Throat Area,	207 cm^2	103 cm^2

Wedge: 20^o Included Angle, 5.08 cm Stroke

Oscillator Frequency: Zero to 15 Hz

Boundary Layer Trips

0.63 mm diameter wires on four walls at test section entrance.

Table 2. Wave Generator Configurations and Related Test Section Flows

Configuration Designation	Use	Nozzle Block Set	Wedge	Measured mean velocity	Unit Reynolds number*	Test section pressure, cm H_2O below atm.
I	Steady Flow	A	20^o, Locked at mid-stroke	45.7 m/s	2.95×10^6/m	10.9
II	Steady Flow	B	None	26.6 m/s	1.72×10^6/m	4.45
III	Oscil-lating Flow	A	20^o, 5.08 cm stroke $f \leq 15$ Hz	44.8 m/s	2.89×10^6/m	-

*Based on measured mean velocity

Table 3. Tabulated results for oscillating flow boundary layer experiment. $f = 4.11$ Hz, $x = 1.66$ m, $U_o = 44.79$ m/s, $U_1 = 4.233$ m/s. $U_1/U_o = 0.0945$, $\overline{\omega} = 0.96$, Wave generator configuration III.

y, inches	$y/\delta^\dagger$	Number of cycles	u_o/U_o	u_1/U_1	ϕ, degrees	Turbulence intensity, %*
0.010	0.0091	400	0.469	0.585	3.47	15.7
0.050	0.0455	400	0.607	0.684	3.88	12.0
0.100	0.0909	400	0.672	0.759	4.70	10.8
0.200	0.182	400	0.732	0.830	5.39	9.35
0.300	0.273	400	0.777	0.895	4.80	8.16
0.400	0.364	400	0.820	0.932	4.39	7.34
0.600	0.545	300	0.888	0.989	3.71	5.58
0.800	0.727	250	0.952	1.036	2.17	3.79
1.000	0.909	250	0.985	1.012	0.68	1.91
1.200	1.091	250	0.994	1.000	-0.18	0.86
1.400	1.273	250	0.992	1.002	-0.04	0.64
1.992	1.811	250	1.000	1.000	0	0.64

†Based on measured steady flow $\delta = 1.10$ inches = 2.8 cm, equation (3a)

*Mean value

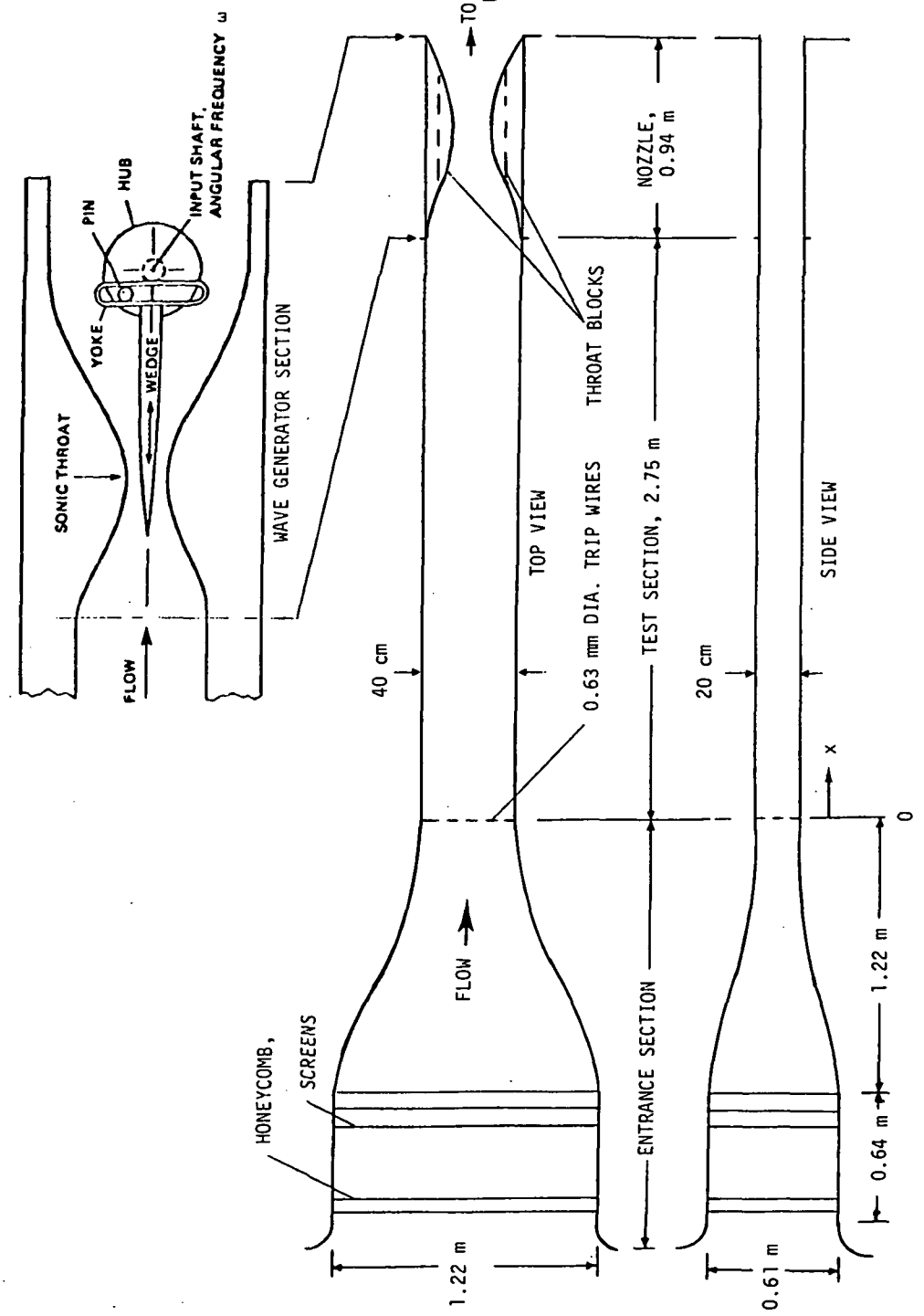

Figure 1. Schematic diagram of the 20 cm x 40 cm oscillating flow tunnel.

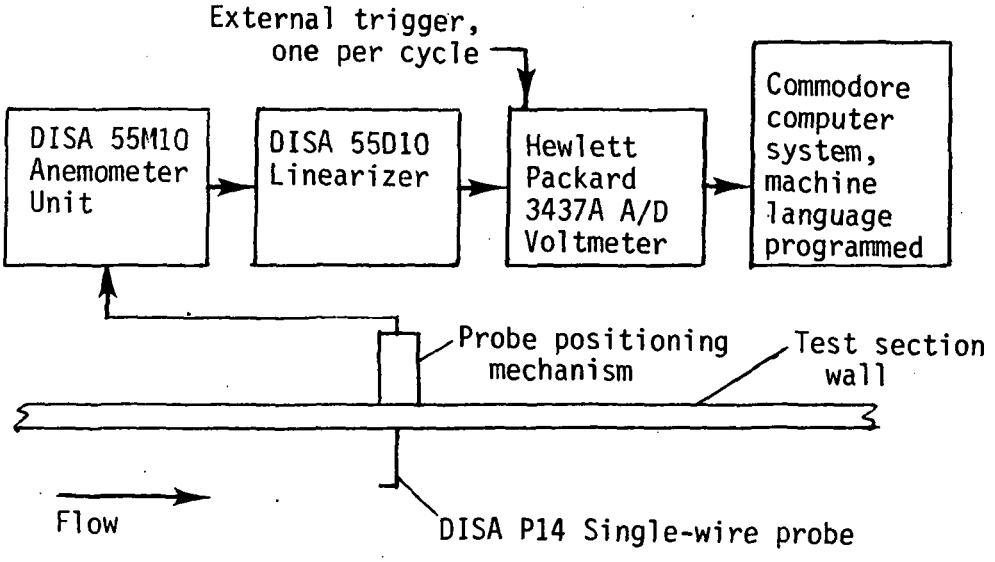

Figure 2. Data Acquisition System.

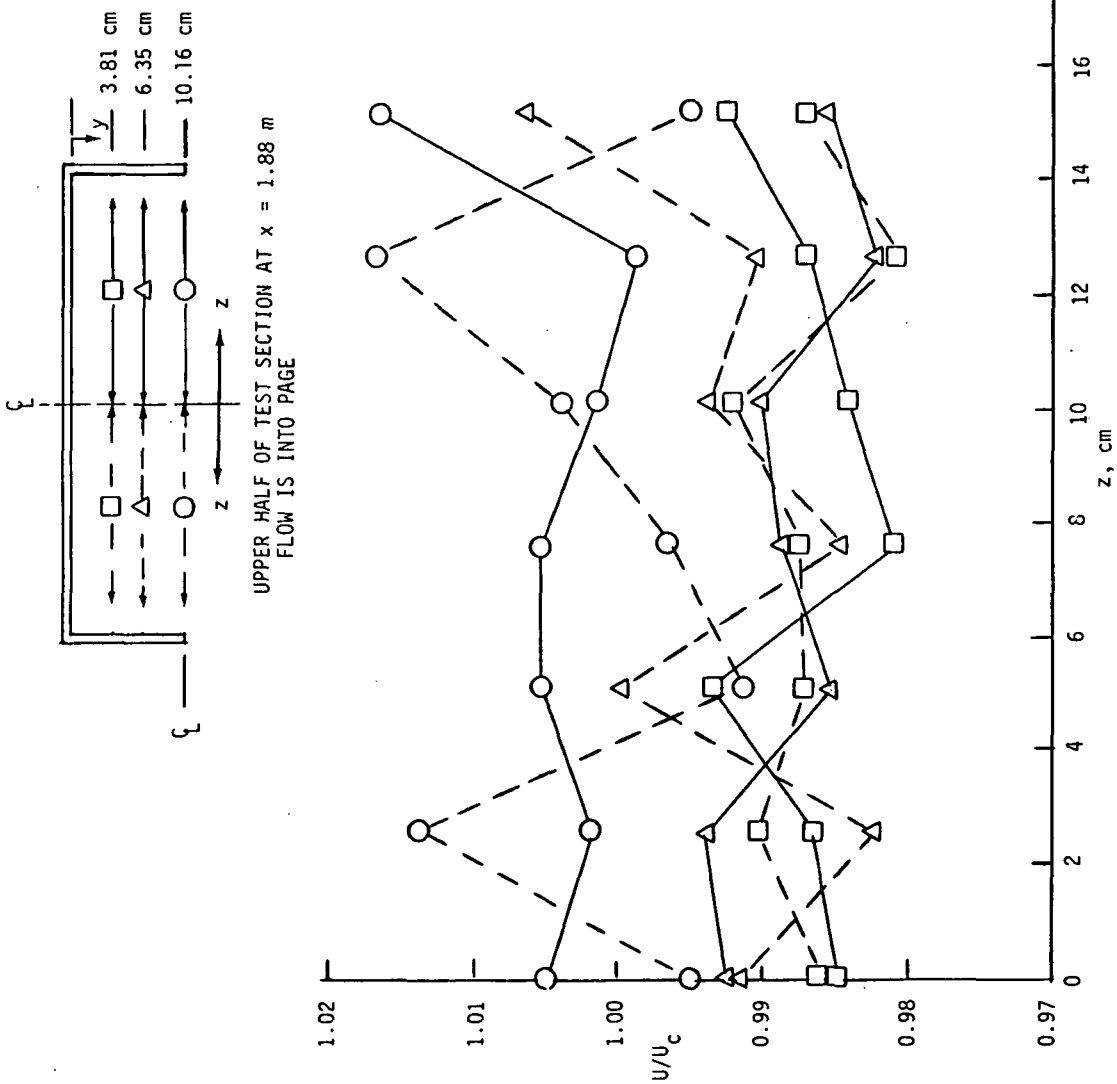

Figure 3. Test section mainstream velocity variation in upper half of cross section at x = 1.88 m. Wave generator configuration I (U = 45.7 m/s).

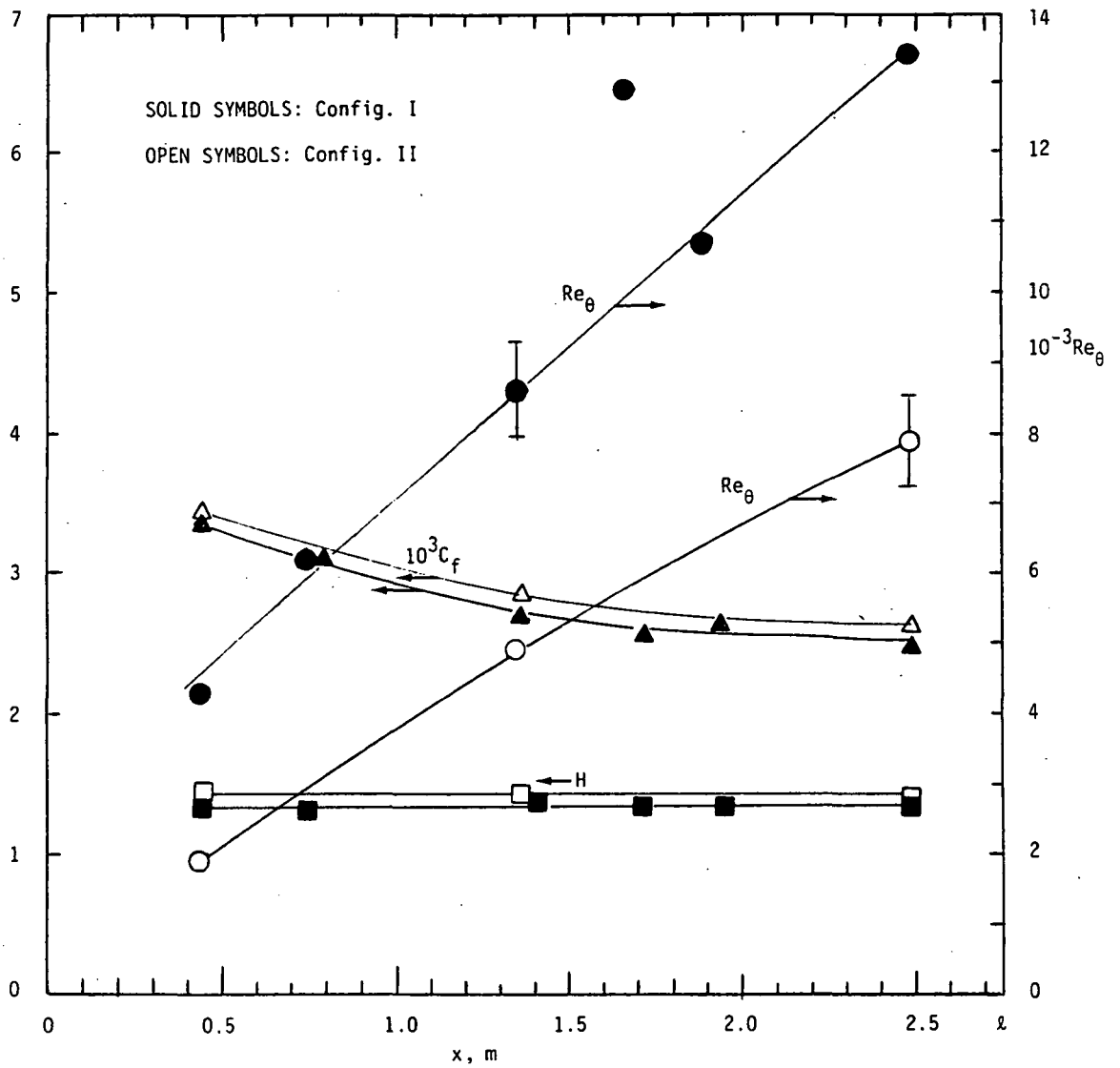

a. Variation of Re_θ, C_f, and H with x.

Figure 4. Boundary layer quantities for steady flows produced by wave generator configuration I, U_o = 45.7 m/s and configuration II, U_o = 26.6 m/s.

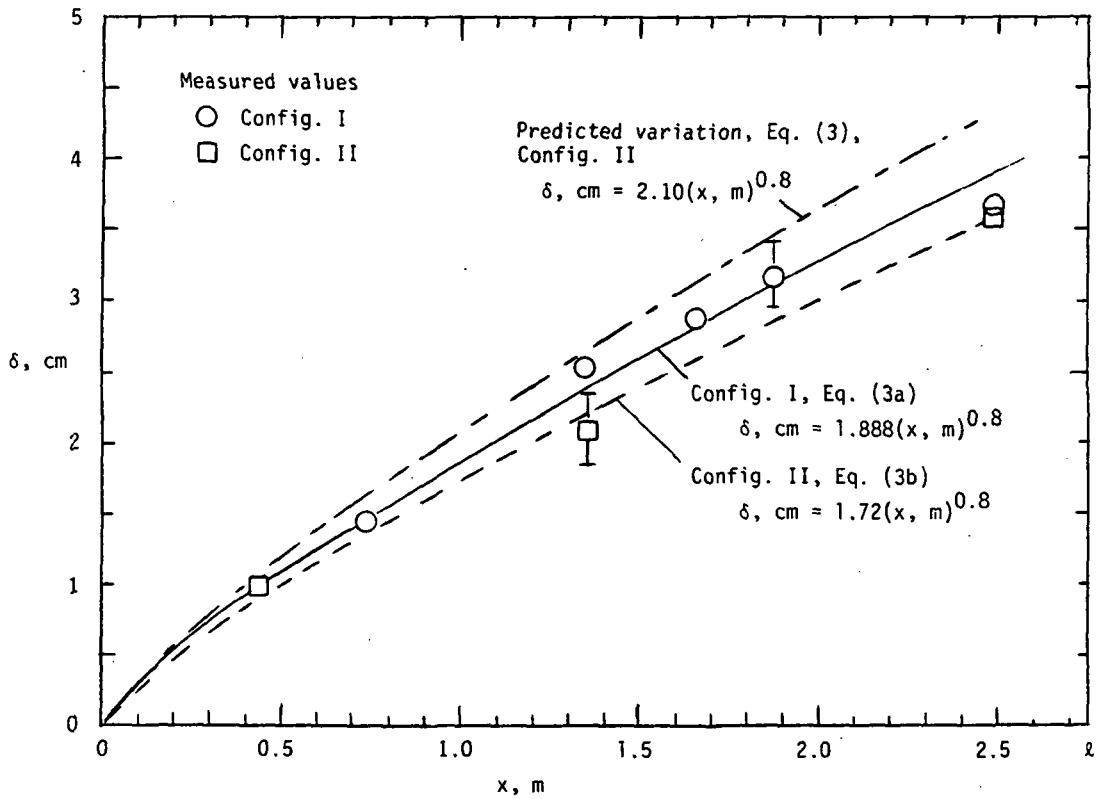

b. Comparisons of predicted and experimental velocity boundary layer thicknesses.

Figure 4. Concluded.

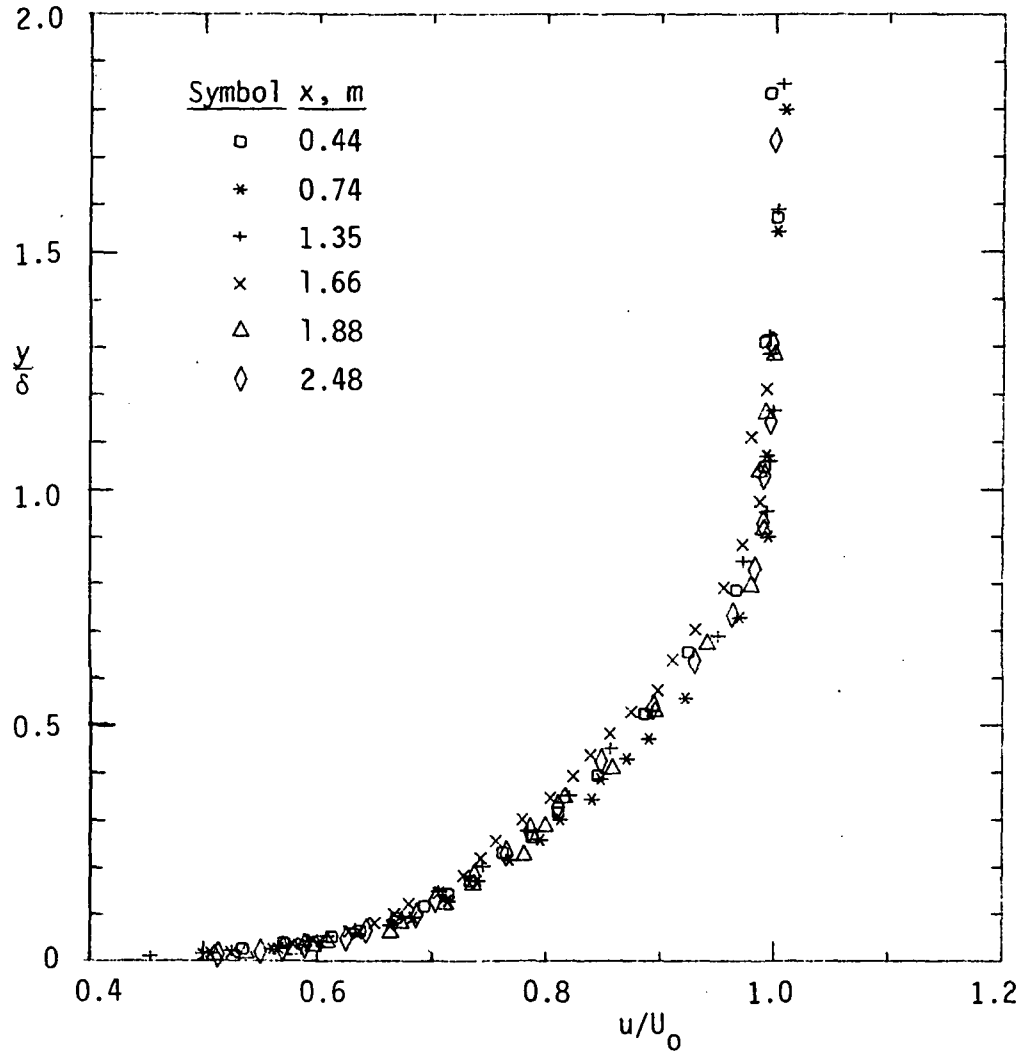

a. Configuration I. U_o = 45.7 m/s.

Figure 5. Steady flow velocity profiles.

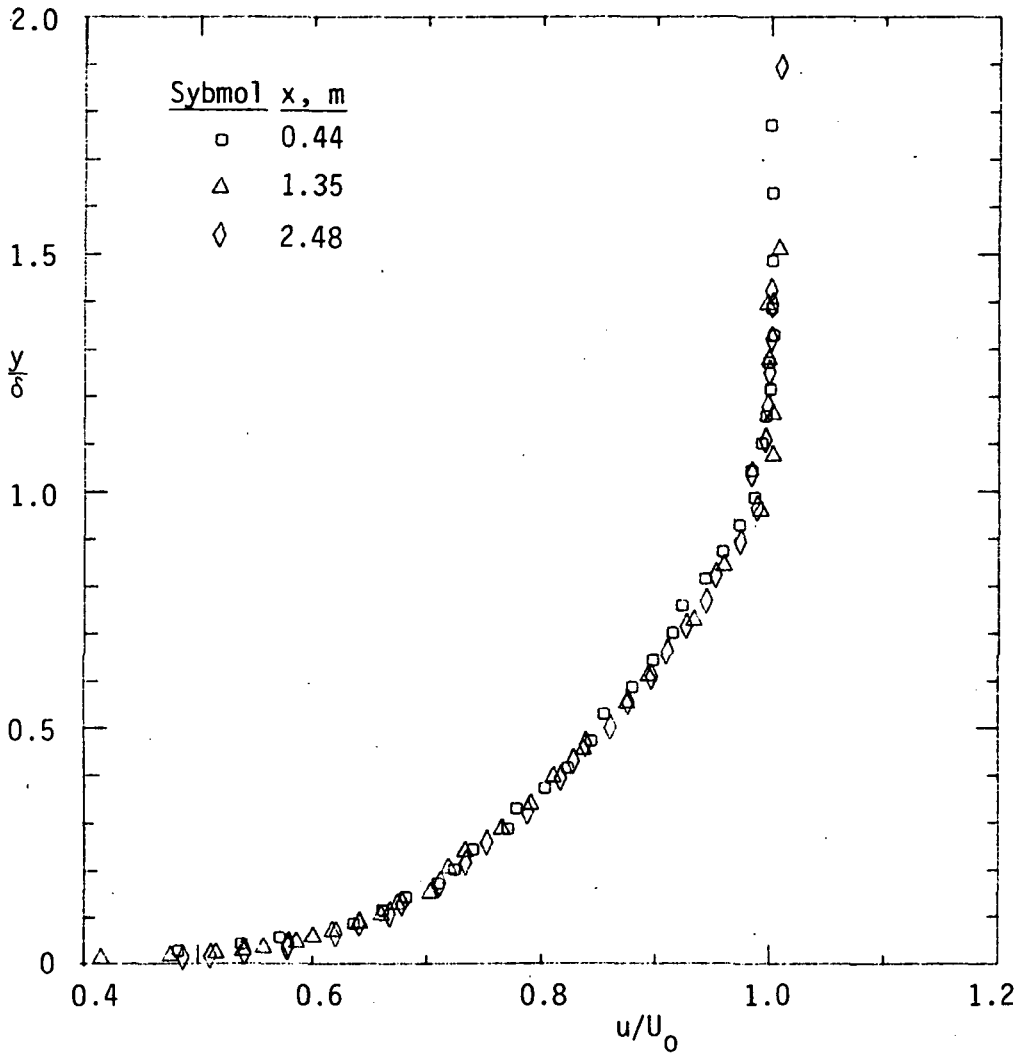

b. Configuration II. U_o = 26.6 m/s.

Figure 5. Continued.

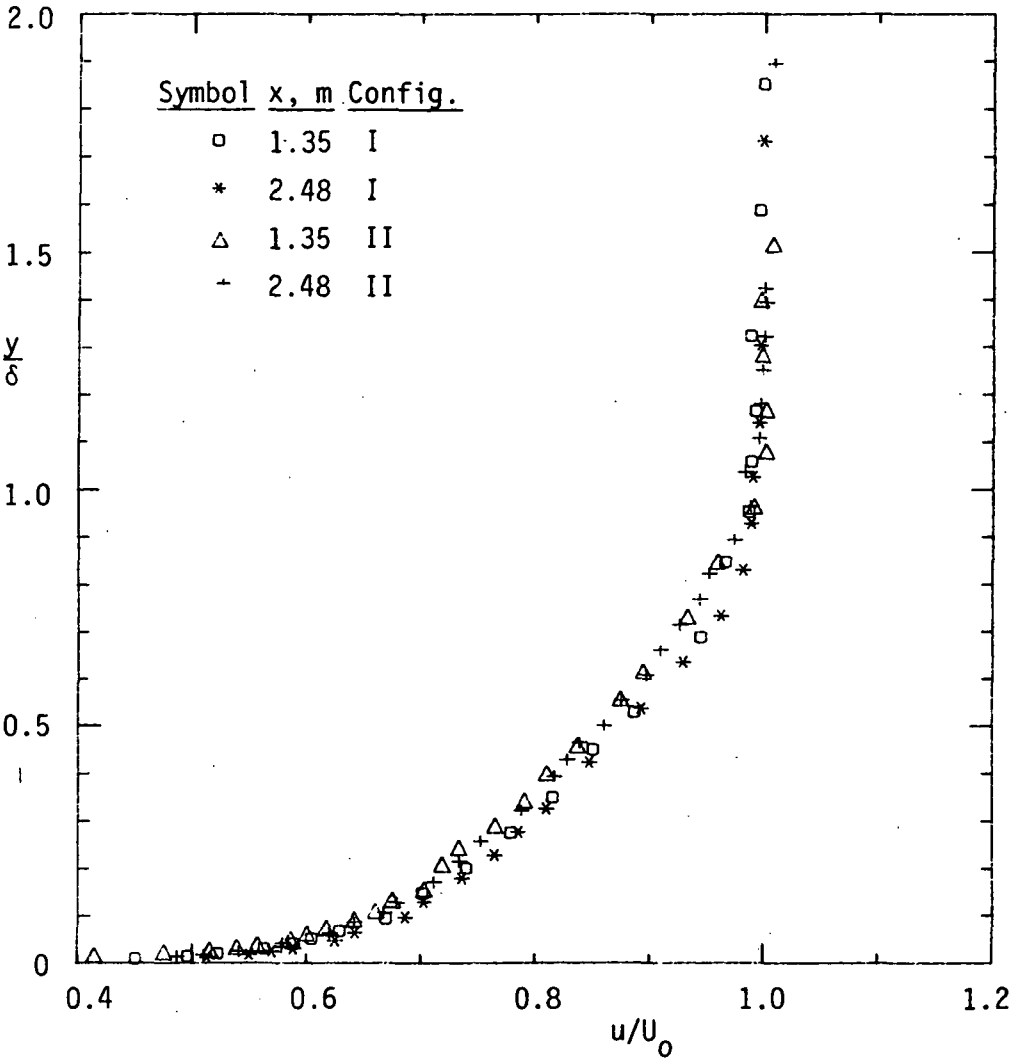

c. Comparison of profiles for configurations I and II.

Figure 5. Concluded.

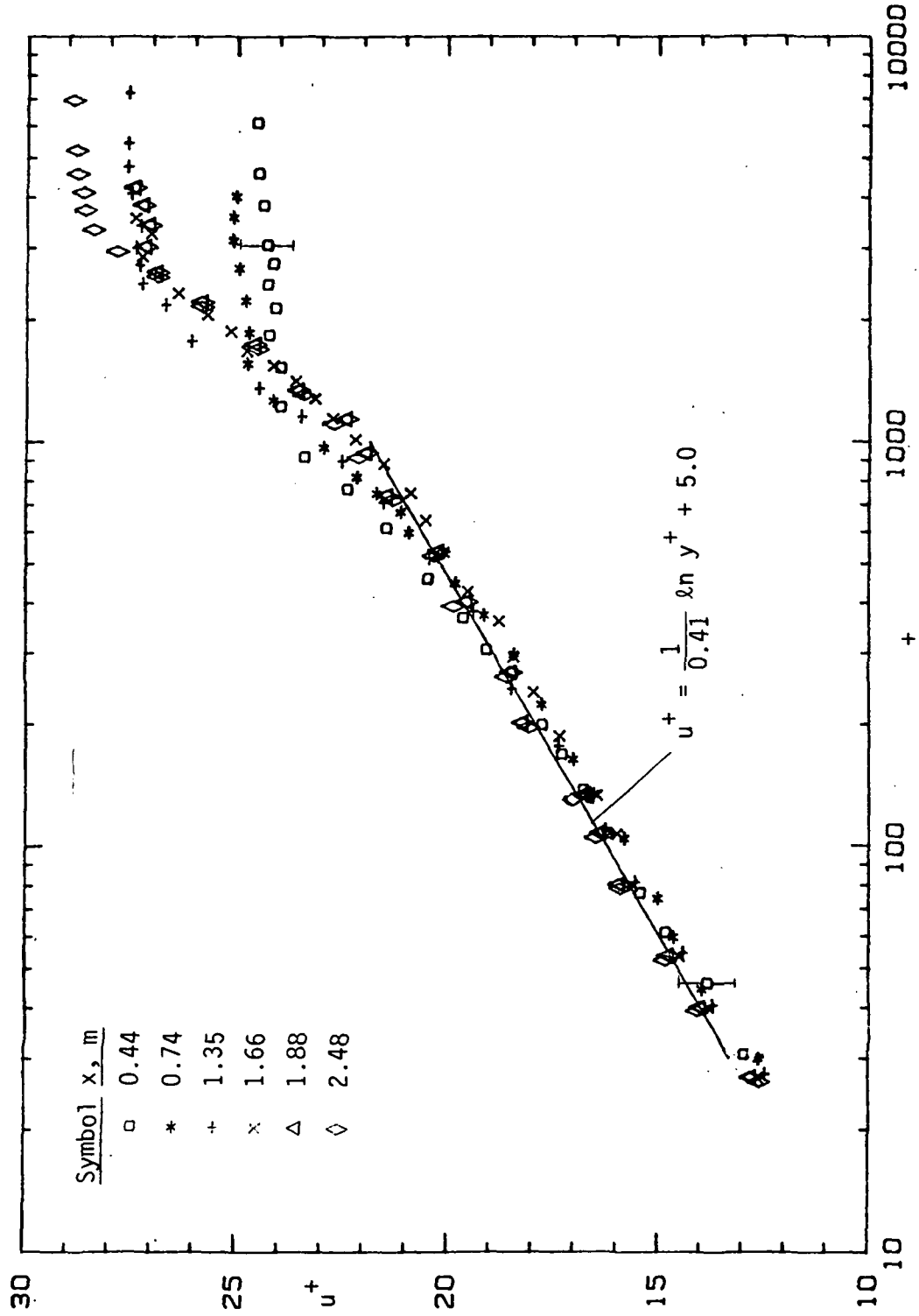

a. Configuration I. U_o = 45.7 m/s.

Figure 6. Velocity profiles in terms of u^+ vs y^+.

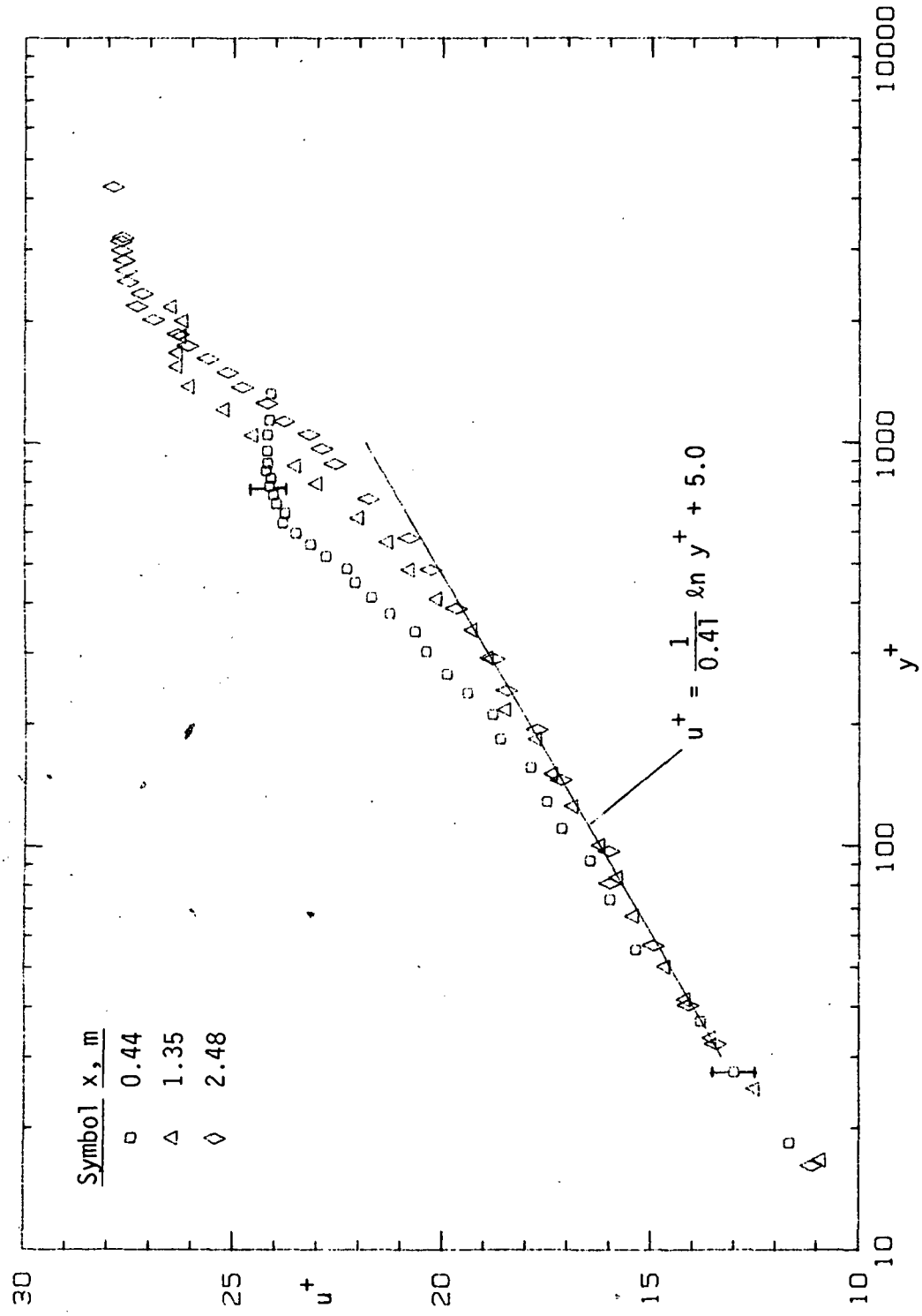

b. Configuration II. U_o = 26.6 m/s.

Figure 6. Concluded.

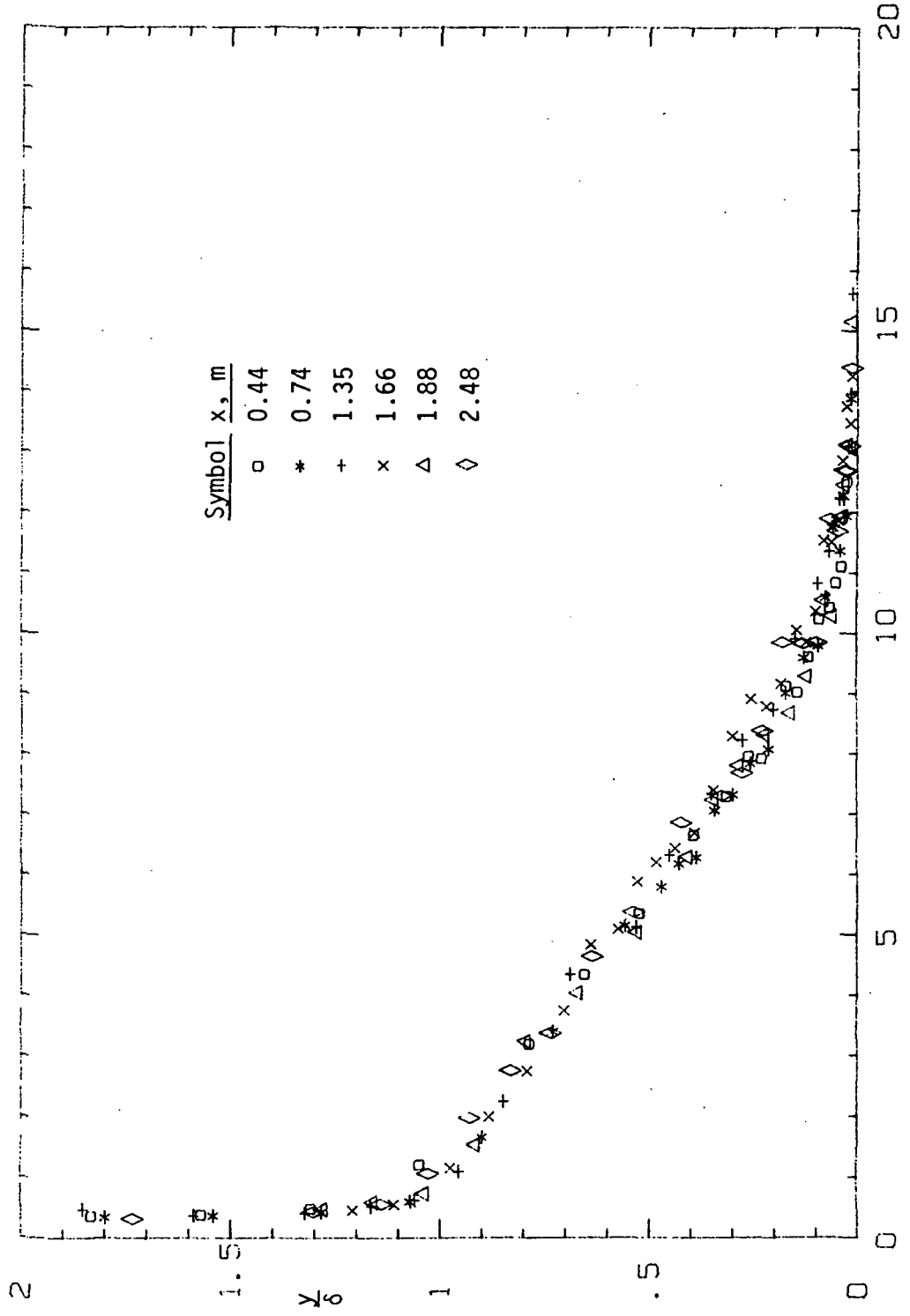

a. Configuration I. U_o = 45.7 m/s.

Figure 7. Turbulence intensities for steady boundary layer flows.

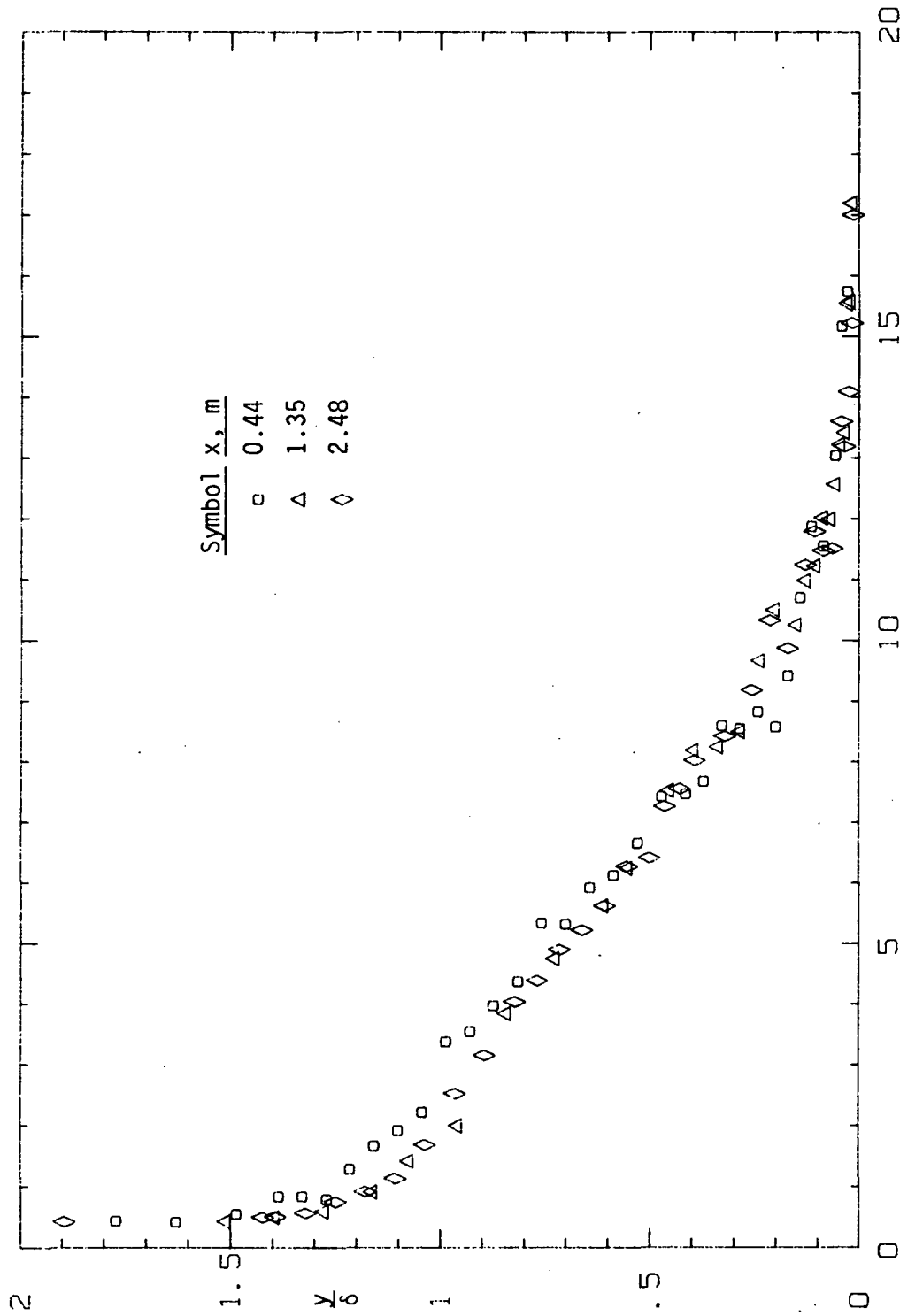

b. Configuration II. U_o = 26.6 m/s.

Figure 7. Continued.

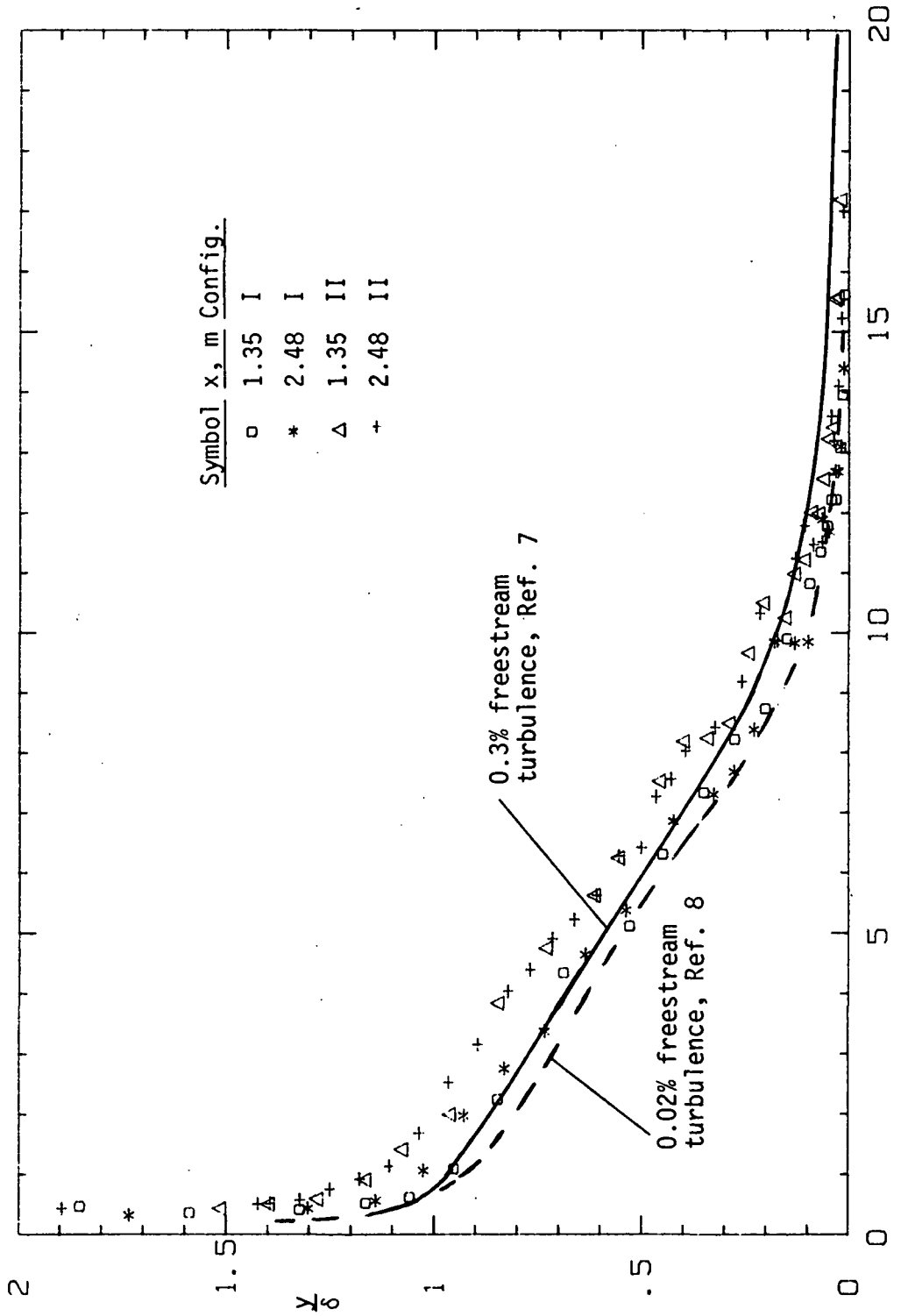

c. Comparisons of turbulence intensities.

Figure 7. Concluded.

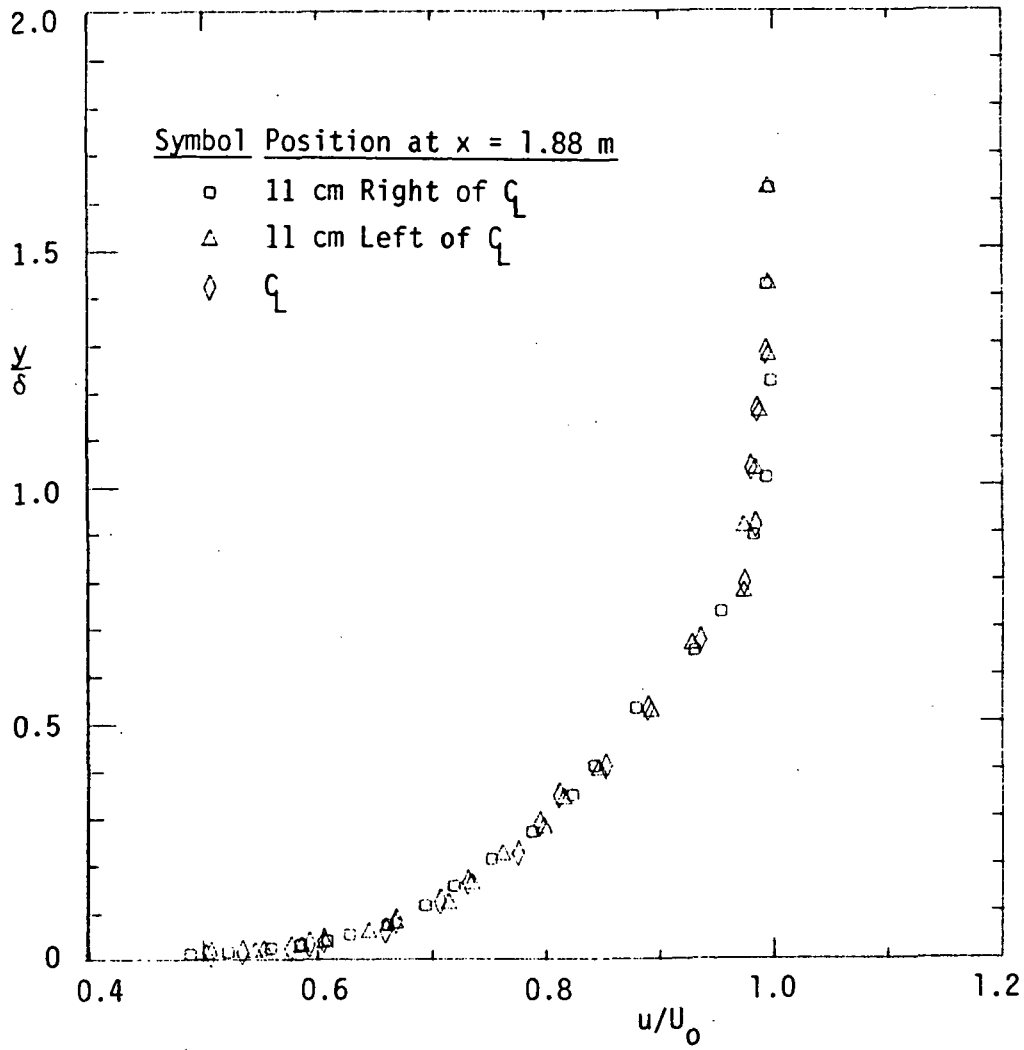

a.

Figure 8. Experimental results for three boundary layer surveys at x = 1.88 m.
(See Figure 3 for left and right designations.)

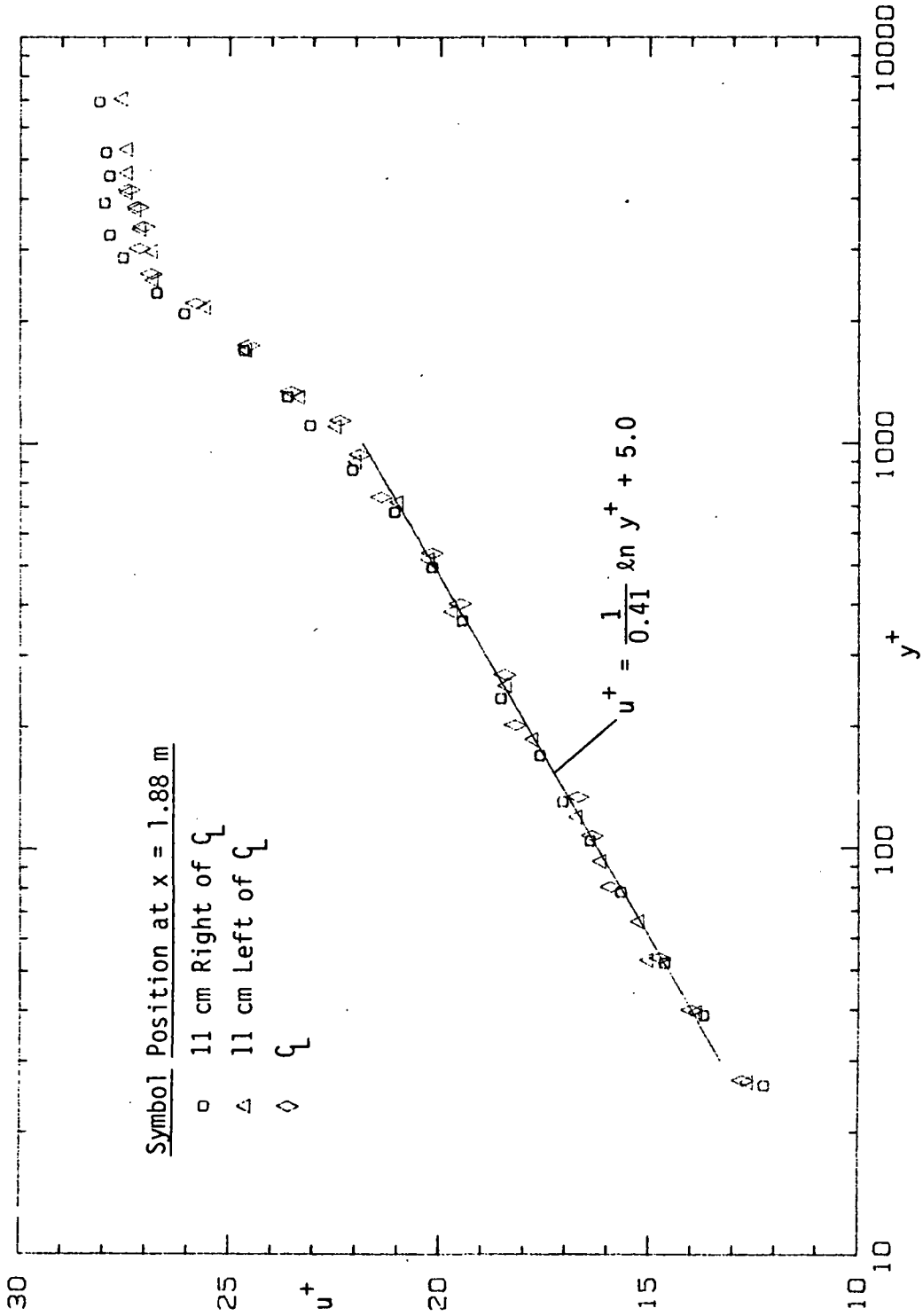

b.

Figure 8. Continued.

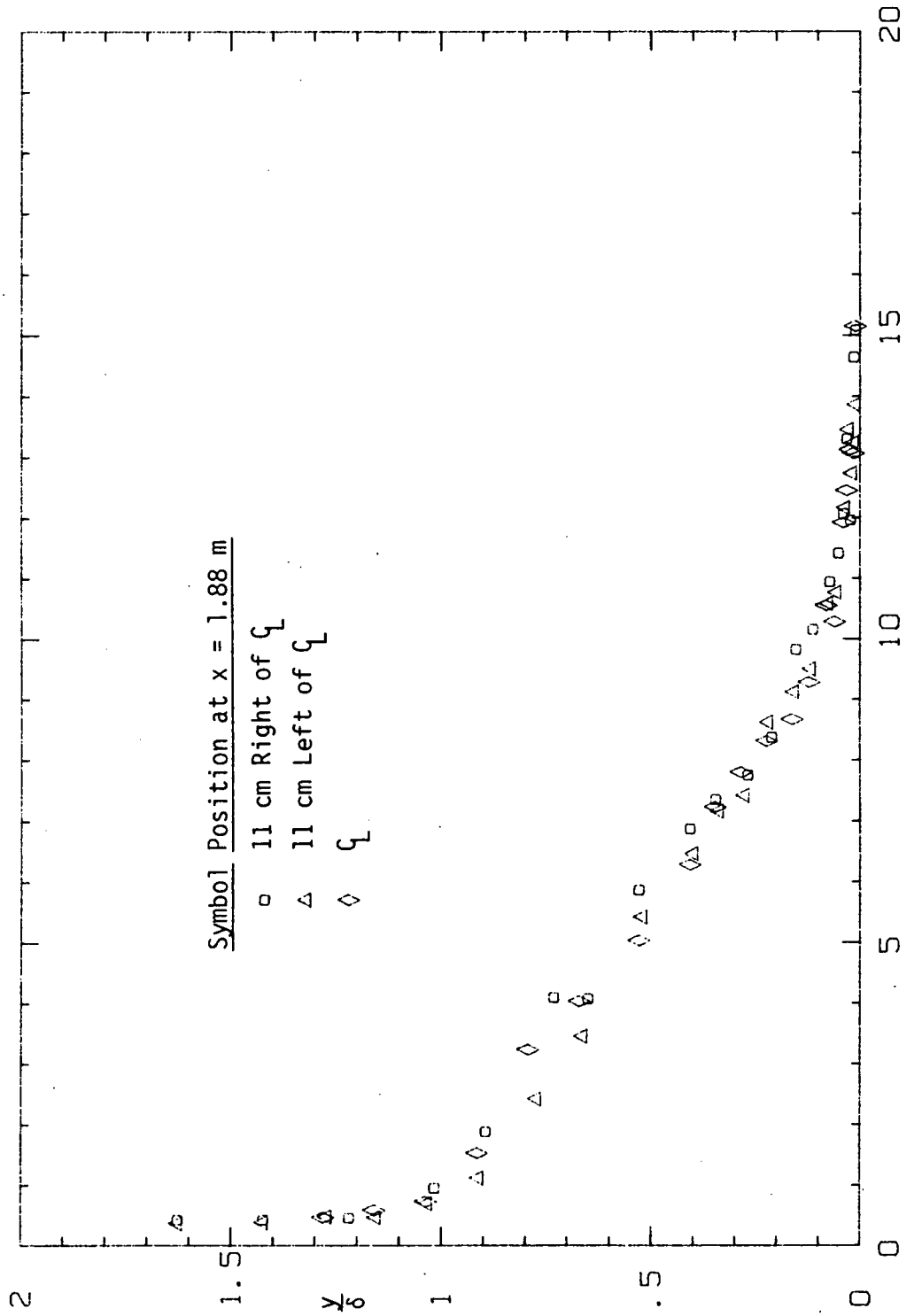

c.

Figure 8. Concluded.

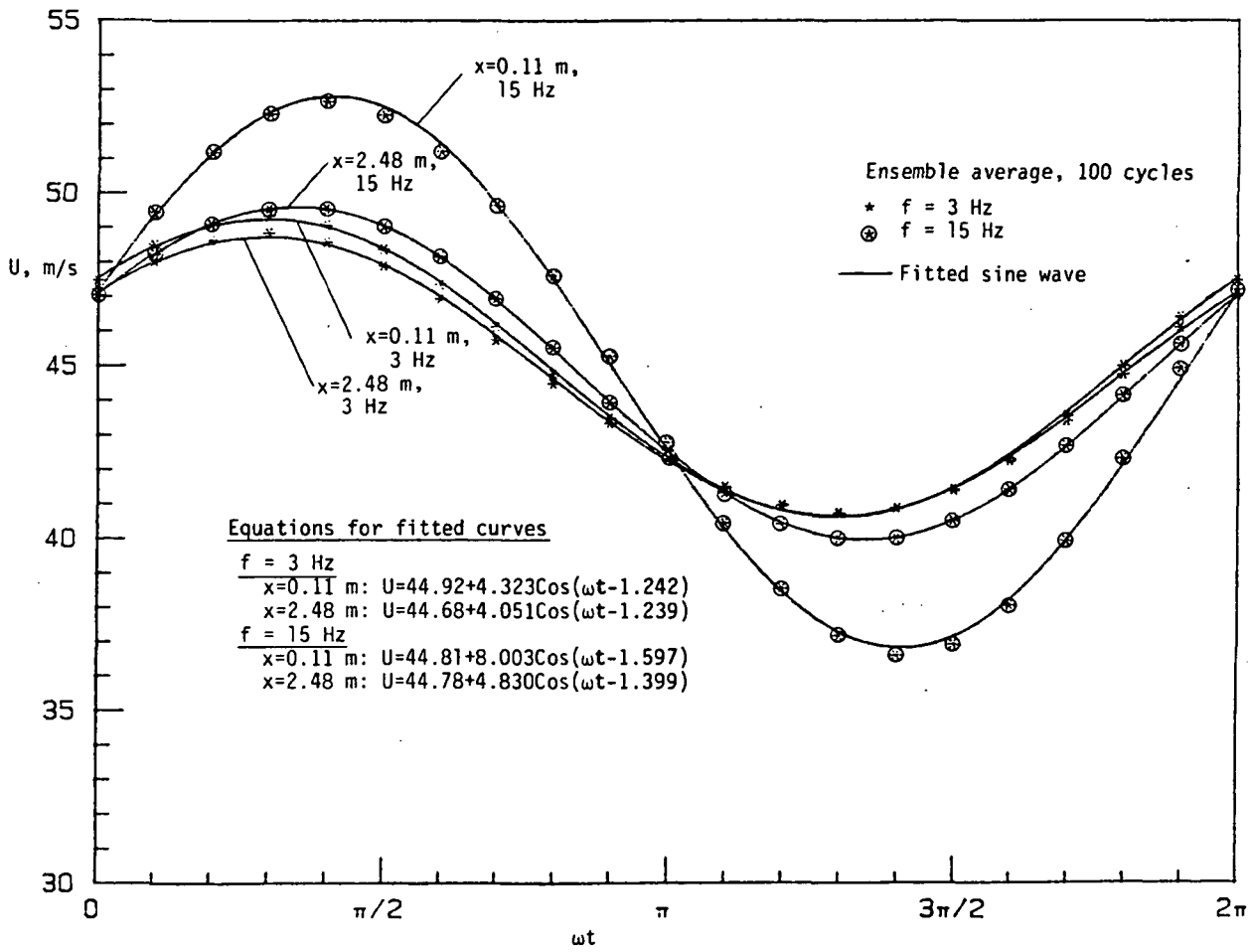

a. Velocity variations at x = 0.11 m and x = 2.48 m for two frequencies.

Figure 9. Results for mainstream oscillating flows.

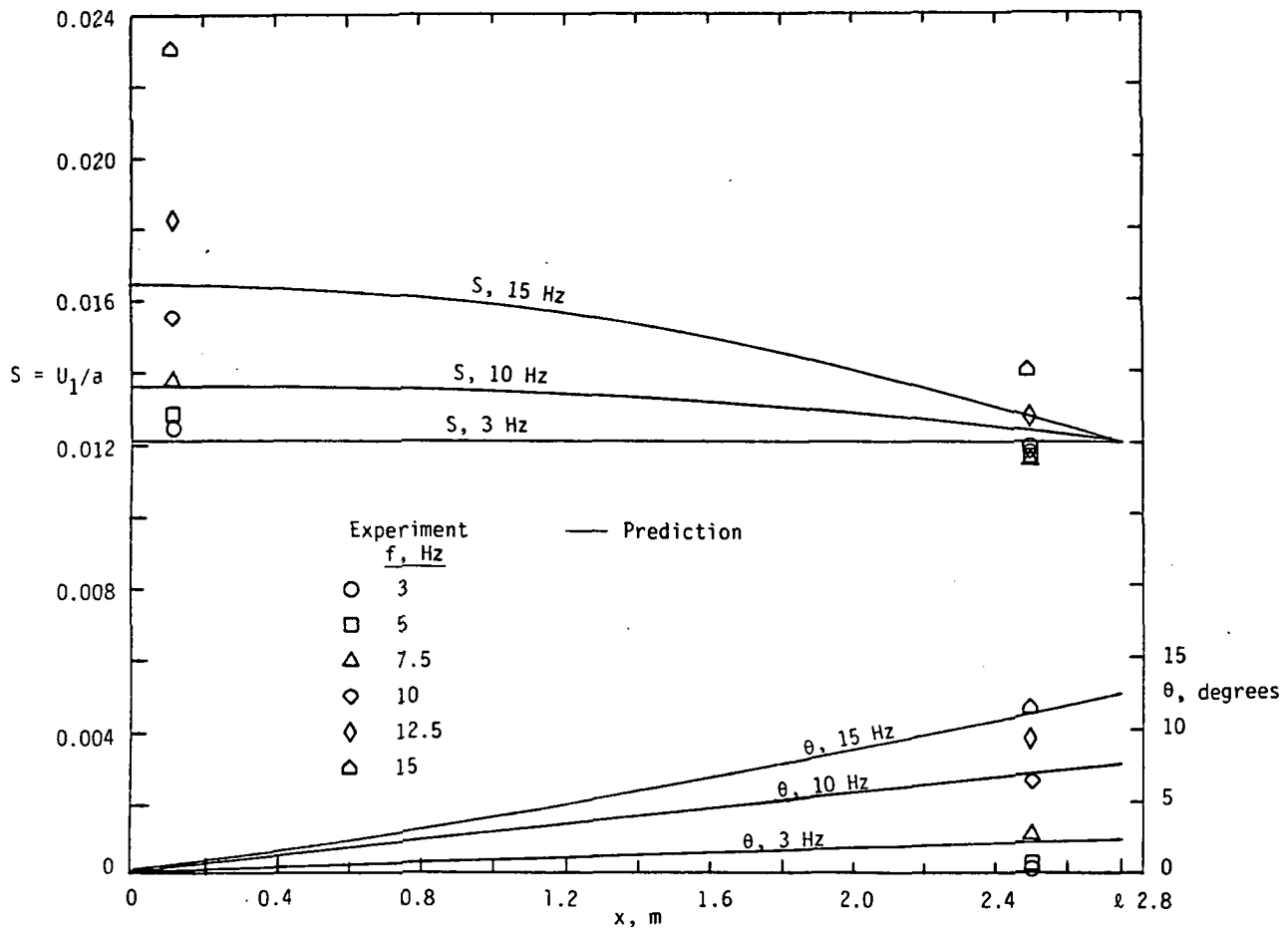

b. Comparisons of experimental and predicted S and θ variations in terms of x.

Figure 9. Continued.

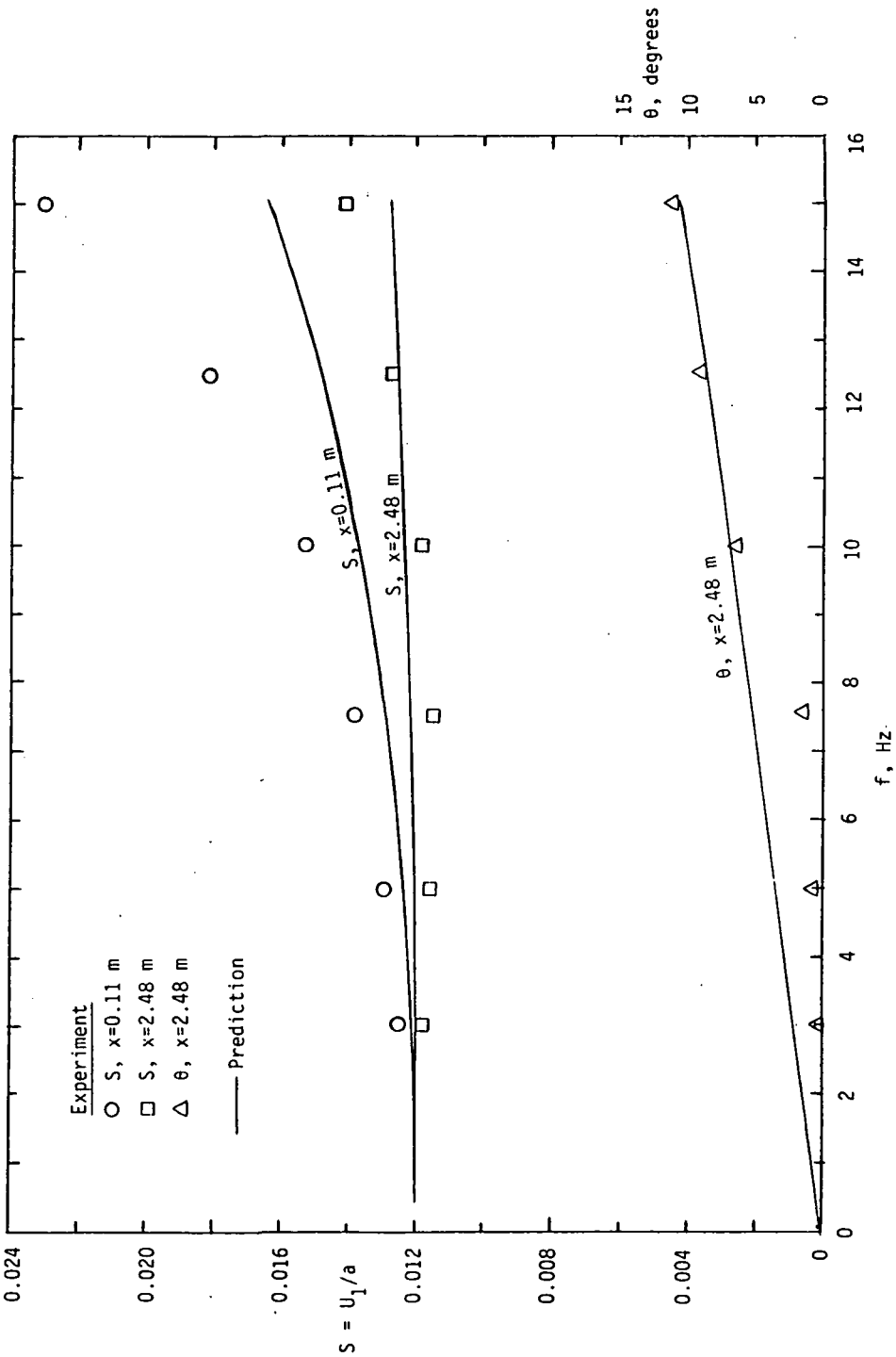

c. Comparisons of experimental and predicted variations of S and θ in terms of frequency for two values of x.

Figure 9. Concluded.

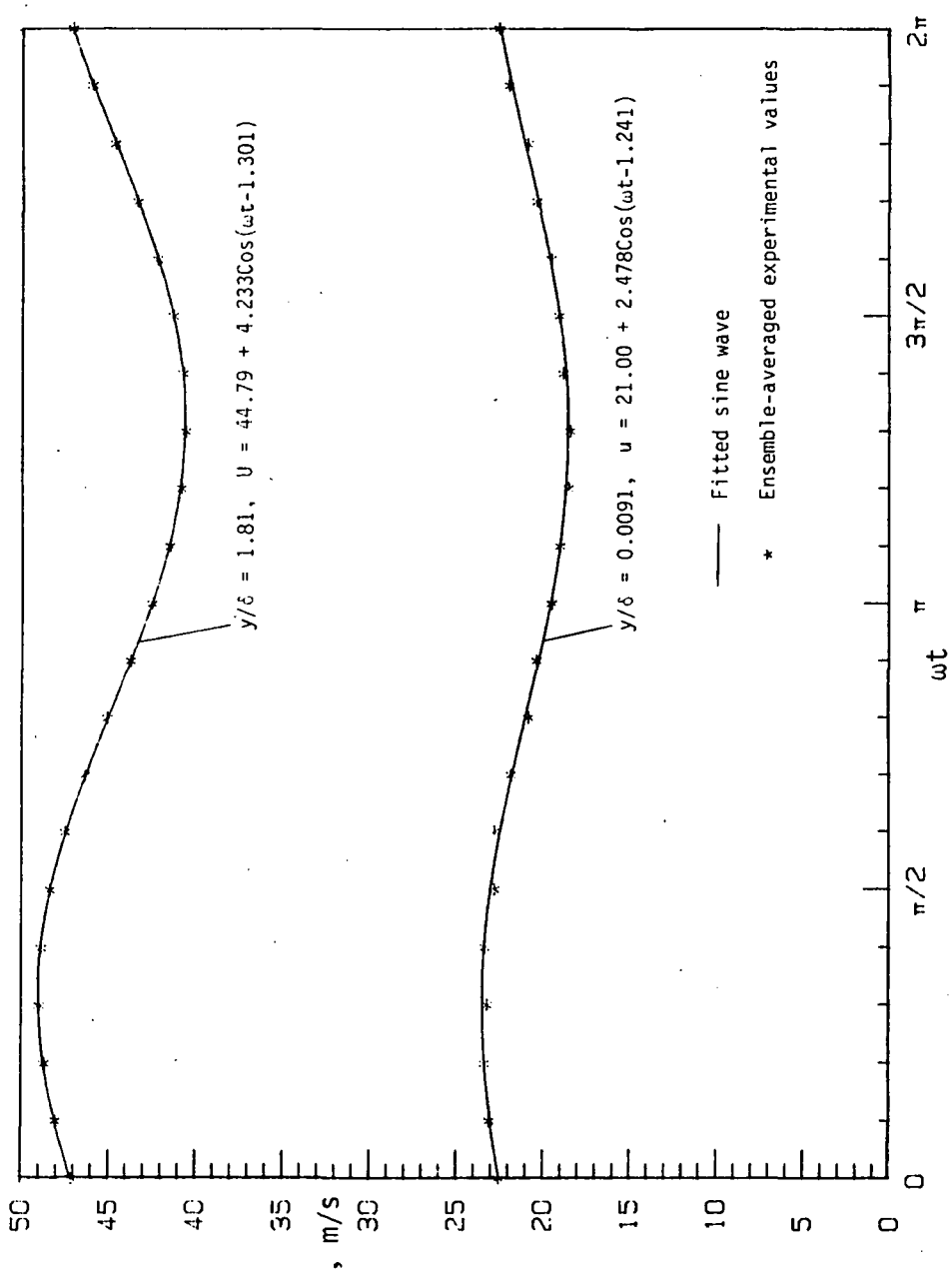

a. Velocity variations at extreme values of y/δ.

Figure 10. Results for oscillating flow boundary layer study.
f = 4.11 Hz, x = 1.66 m.

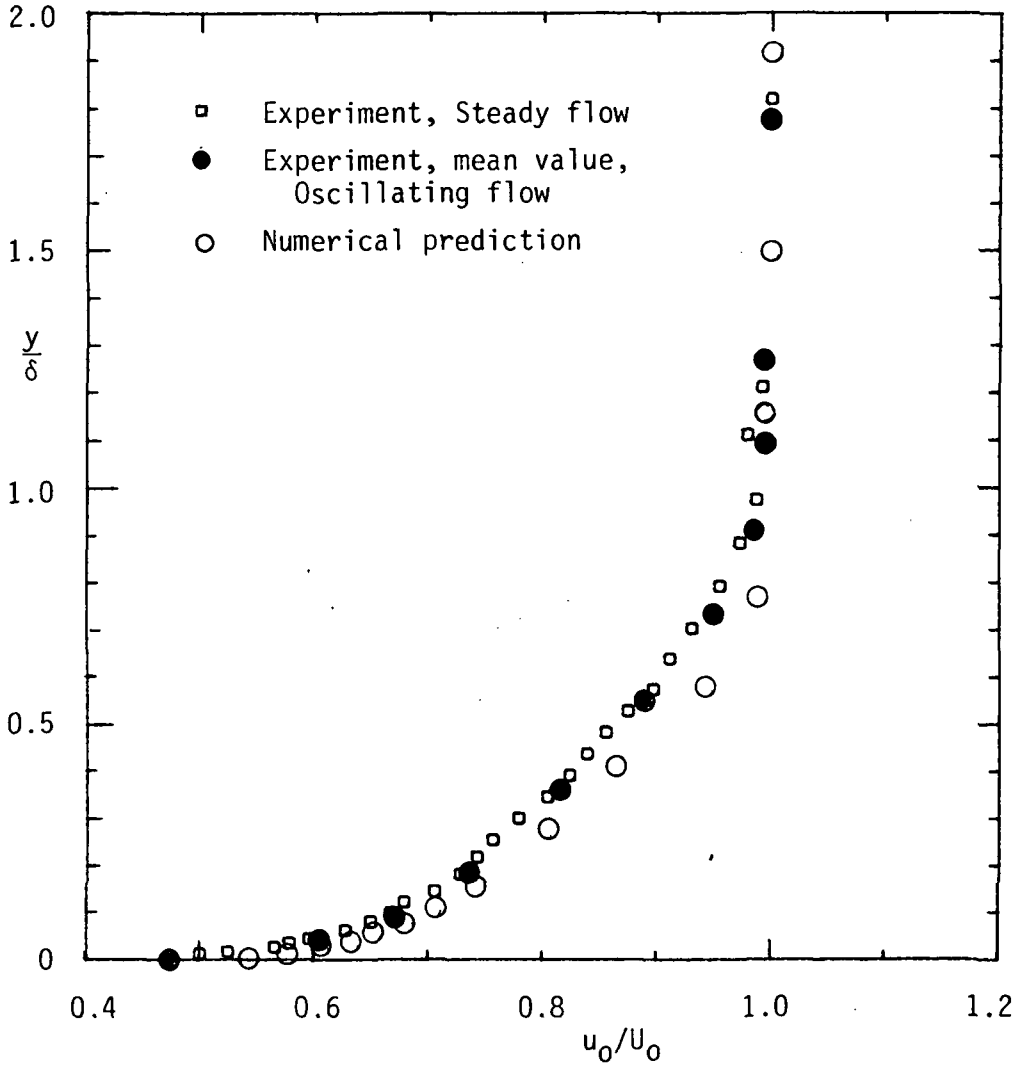

b. Comparison of mean velocity profiles.

Figure 10. Continued.

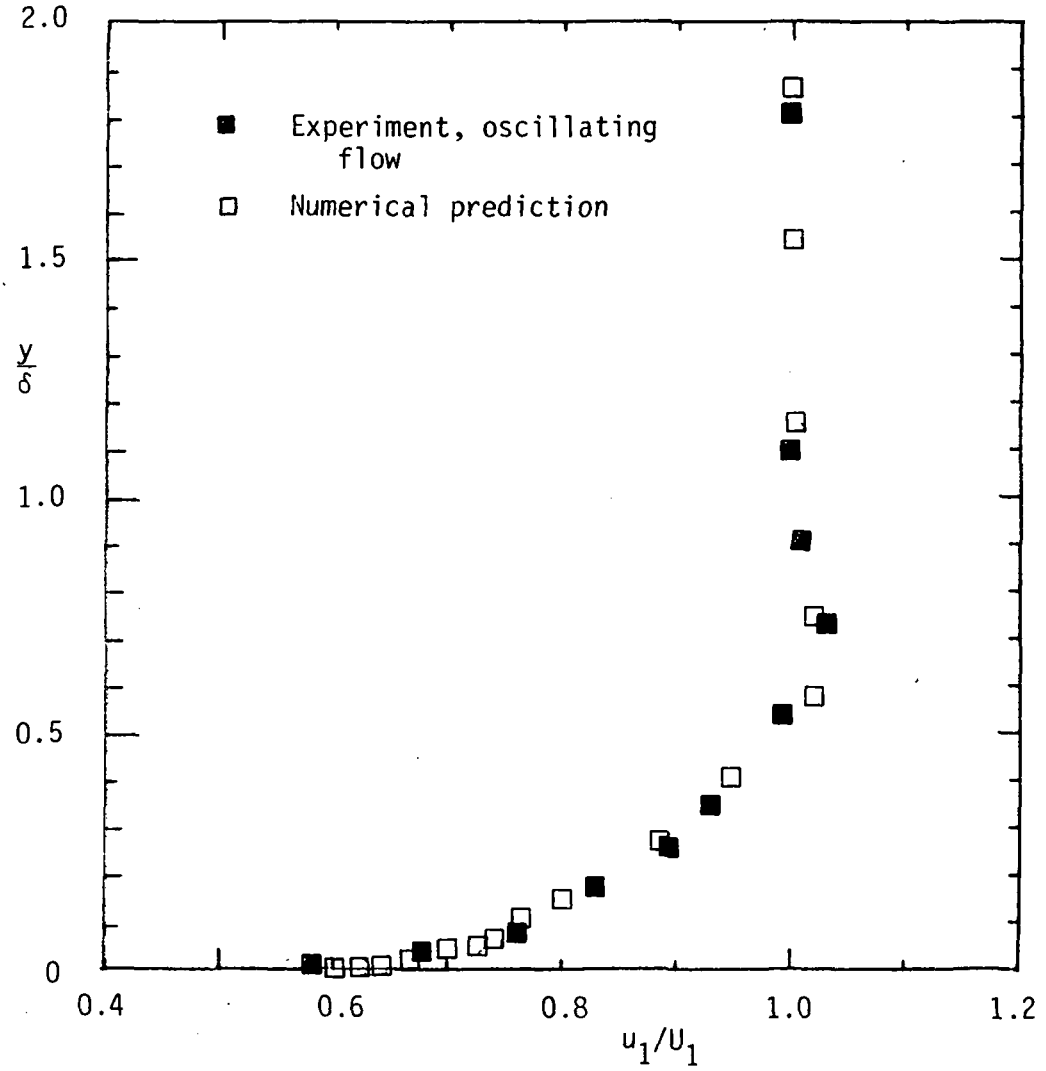

c. Comparison of amplitude ratio profiles.

Figure 10. Continued.

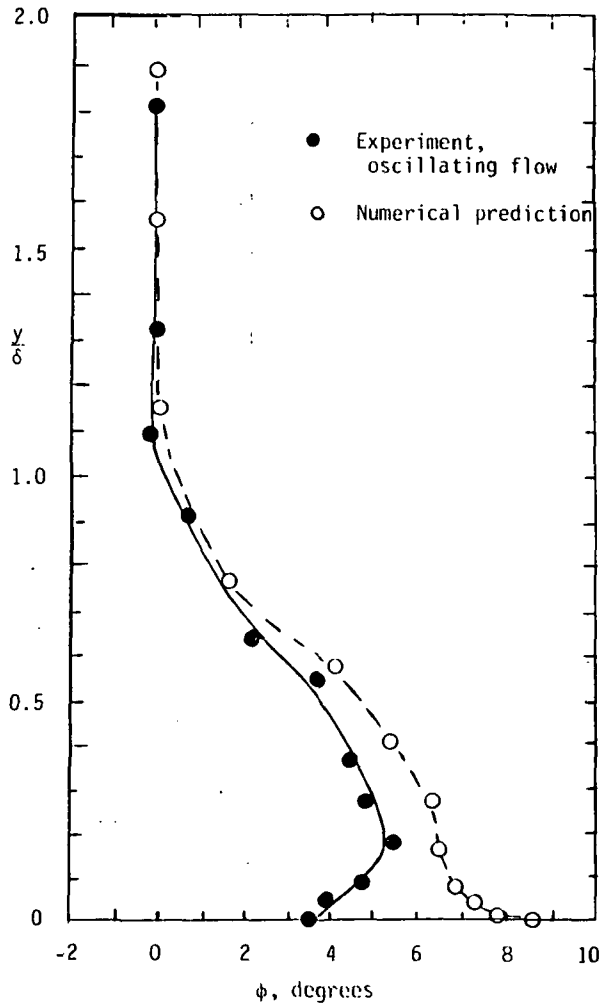

d. Comparison of phase angle profiles

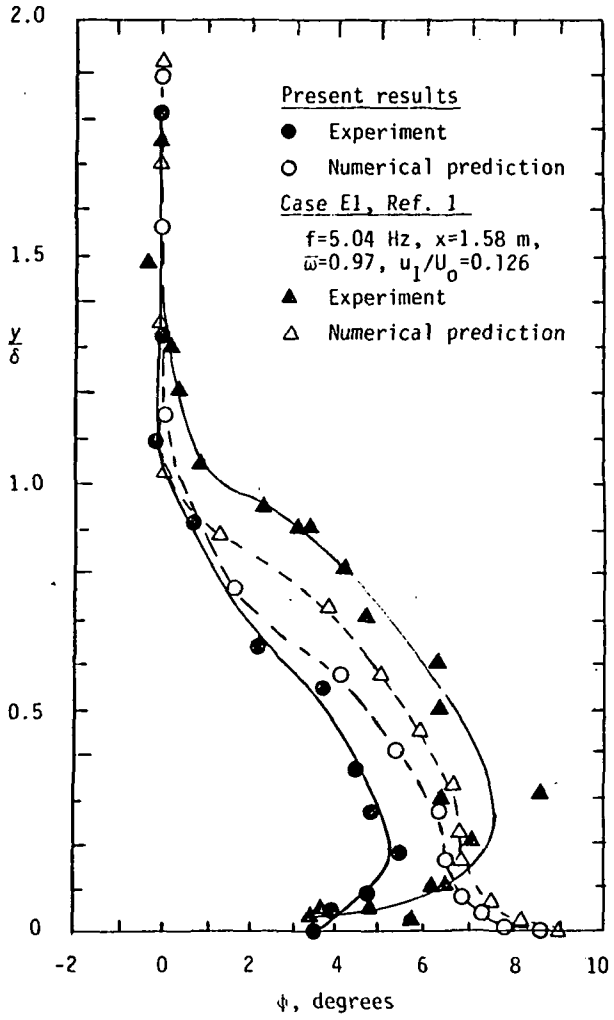

e. Comparisons of results for phase angle for two flow cases.

Figure 10. Continued.

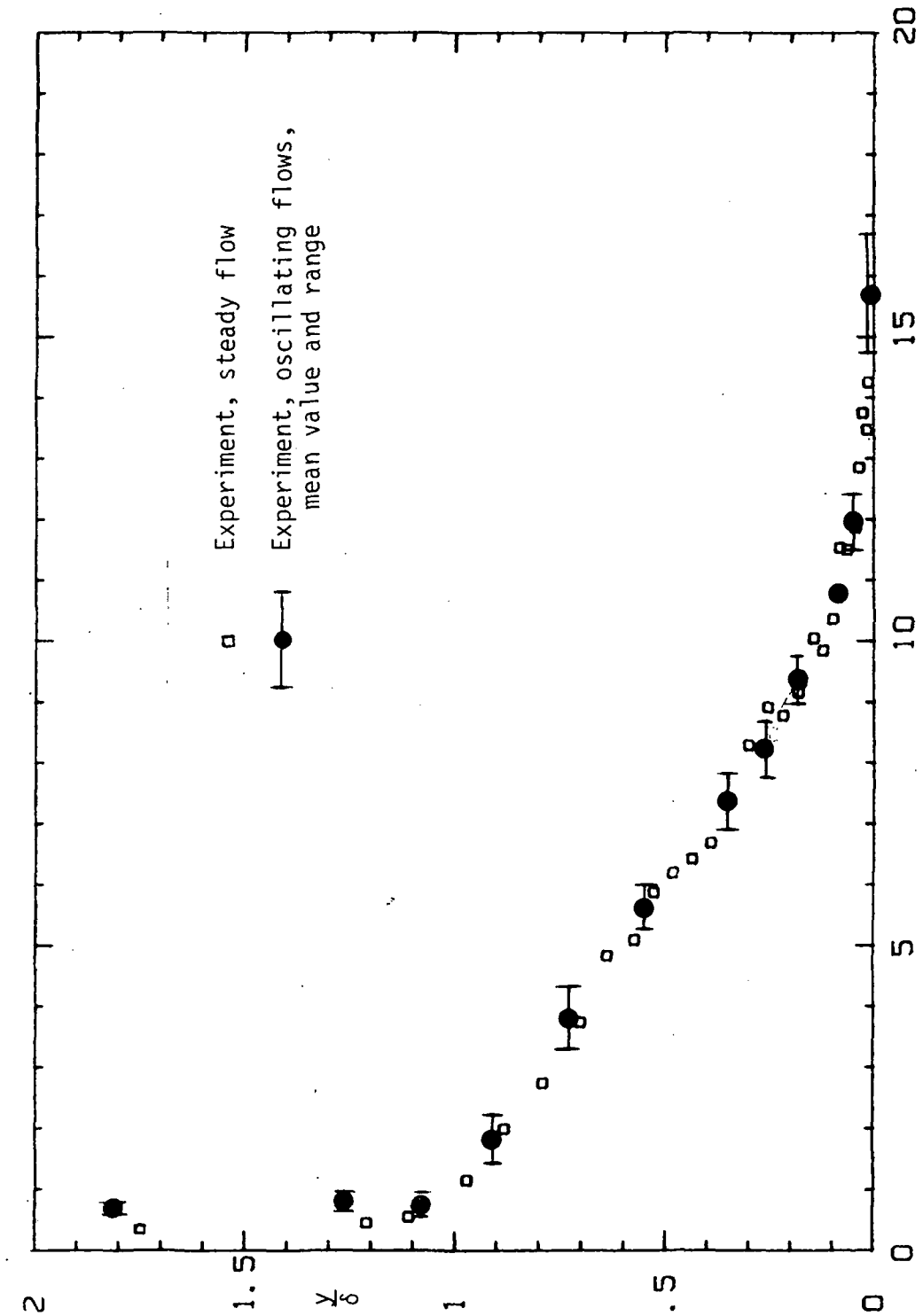

f. Comparison of turbulence intensities for steady and oscillating flows.

Figure 10. Concluded.